

# ANTIBODIES FOR SEROLOGY AND DIAGNOSTICS



W Anti-Human IgE Antibodies  
E For high-specificity immunoassay  
Z design and performance



[Learn more](#)

## Research Article

# Antibody isotype epitope mapping of SARS-CoV-2 Spike RBD protein: Targets for COVID-19 symptomatology and disease control

Marinela Contreras<sup>1,2</sup>, Joaquín Vicente<sup>1</sup>, José Joaquín Cerón<sup>2</sup>,  
Silvia Martínez Subiela<sup>2</sup>, José Miguel Urrea<sup>3,4</sup> ,  
Francisco J. Rodríguez-del-Río<sup>1,5</sup>, Elisa Ferreras-Colino<sup>1</sup>,  
Rita Vaz-Rodrigues<sup>1</sup>, Isabel G. de Fernández de Mera<sup>1</sup>, Sandra Antunes<sup>6,7</sup>,  
Ana Domingos<sup>6,7</sup>, Christian Gortázar<sup>1</sup> and José de la Fuente<sup>1,8</sup> 

<sup>1</sup> SaBio, Instituto de Investigación en Recursos Cinegéticos IREC-CSIC-UCLM-JCCM, Ronda de Toledo s/n, Ciudad Real, Spain

<sup>2</sup> Interdisciplinary Laboratory of Clinical Analysis, Interlab-UMU, Regional Campus of International Excellence Campus Mare Nostrum, University of Murcia, Murcia, Espinardo, Spain

<sup>3</sup> Immunology, Hospital General Universitario de Ciudad Real, Ciudad Real, Spain

<sup>4</sup> Medicine School, Universidad de Castilla la Mancha (UCLM), Ciudad Real, Spain

<sup>5</sup> Local Medical Service Horcajo de los Montes, Ciudad Real, Spain

<sup>6</sup> Instituto de Higiene e Medicina Tropical, Universidade Nova de Lisboa, Lisboa, Portugal

<sup>7</sup> Global Health and Tropical Medicine, Instituto de Higiene e Medicina Tropical, Universidade Nova de Lisboa (GHTM-IHMT-UNL), Lisboa, Portugal

<sup>8</sup> Department of Veterinary Pathobiology, Center for Veterinary Health Sciences, Oklahoma State University, Stillwater, Oklahoma, USA

Severe acute respiratory syndrome coronavirus 2 (SARS-CoV-2) still poses a challenge for biomedicine and public health. To advance the development of effective diagnostic, prognostic, and preventive interventions, our study focused on high-throughput antibody binding epitope mapping of the SARS-CoV-2 spike RBD protein by IgA, IgM and IgG antibodies in saliva and sera of different cohorts from healthy uninfected individuals to SARS-CoV-2-infected unvaccinated and vaccinated asymptomatic, recovered, nonsevere, and severe patients. Identified candidate diagnostic (455-LFRKSNLKPFERD-467), prognostic (395-VYADSFVIRGDEV-407-C-KLH, 332-ITNLCPFGEV-342-C-KLH, 352-AWNRKRI-358-C-KLH, 524-VCGPKKSTNLVKN-536-KLH), and protective (MKLLE-487-NCYFPLQSYGFQPTNGVG-504-GGGGS-446-GGNYNYLYRLFRKSNLKPFERD-467) epitopes were validated with sera from prevaccine and postvaccine cohorts. The results identified neutralizing epitopes and support that antibody recognition of linear B-cell epitopes in RBD protein is associated with antibody isotype and disease symptomatology. The findings in asymptomatic individuals suggest a role for anti-RBD antibodies in the protective response against SARS-CoV-2. The possibility of translating results into diagnostic interventions for the early diagnosis of asymptomatic individuals and prognosis

**Correspondence:** José de la Fuente  
e-mail: jose\_delafuente@yahoo.com; josedejesus.fuente@uclm.es

of disease severity provides new tools for COVID-19 surveillance and evaluation of risks in hospitalized patients. These results, together with other approaches, may contribute to the development of new vaccines for the control of COVID-19 and other coronavirus-related diseases using a quantum vaccinomics approach through the combination of protective epitopes.

**Keywords:** antibody isotype · epitope mapping · prognostic, SARS-CoV-2 · spike protein



Additional supporting information may be found online in the Supporting Information section at the end of the article.

## Introduction

Infection with severe acute respiratory syndrome coronavirus 2 (SARS-CoV-2) resulted in coronavirus disease 2019 (COVID-19), a pandemic with asymptomatic cases and patients recovered at hospital discharge, nonsevere hospitalized and severe in the intensive care unit (ICU) [1–4]. Vaccines constitute the safest and most effective intervention for the control of COVID-19, with a reduction in infected and mostly asymptomatic cases [5, 6]. However, the circulation of new SARS-CoV-2 genetic variants in both vaccinated and unvaccinated individuals causes different disease symptomatology and constitutes a challenge for disease prevention and control [4, 7–9].

The SARS-CoV-2 spike (S) protein plays an essential role in virus binding and infection of host cells and thus constitutes the primary target for therapeutic and vaccine interventions [10]. The S protein ectodomain is composed of the S1 subunit with the N-terminal and receptor binding domain (RBD) and the S2 subunit with the fusion domain mediating entry into host cells [11]. The RBD initiates virus attachment through interaction with the angiotensin-converting enzyme 2 (ACE2) receptor [12–14]. The functional significance of the ACE2-RBD interaction makes the RBD a prime target for neutralizing antibodies [15–17]. Targeting this domain increases the selective pressure on the RBD, which may promote the emergence of escape mutants that maintain virulence [18–21]. Indeed, neutralizing antibodies targeting a single epitope can induce virus escape in cell culture, quickly rendering antibodies ineffective [22], and thus targeting multiple nonoverlapping RBD epitopes is more effective for SARS-CoV-2 neutralization [18, 22–26].

Therefore, the identification of B-cell epitopes in the SARS-CoV-2 S protein is essential for the development of effective diagnostic and prognostic tests, therapeutic interventions, and vaccines. For example, the identified N3-1 antibody with high affinity (equilibrium dissociation constant  $K_d = 68$  pM) to the RBD shows a high *in vitro* SARS-CoV-2 neutralization capacity [27]. Mapping of B-cell linear epitopes of the SARS-CoV-2 RBD using different methodological approaches has shown binding of IgA and IgG antibodies with potential neutralizing capacity [28]. However, a poor reaction of RBD epitopes with COVID-19 sera has been reported [29, 30]. A control experiment with the AI334/CR3022 antibody documented a weak reaction

with the 367-VLYNSASFSTFK-378 RBD epitope [16, 31]. Other identified epitopes have shown low specificity to COVID-19 sera [32], including reactive epitopes in peptide arrays with COVID-19 patient sera but are not significantly different from healthy controls [33] (Table 1). In some experiments, IgM responses against the S protein were not different between symptomatic COVID-19 patients and healthy individuals or lung cancer patients and uninfected controls [32]. However, recent results showed recognition of RBD linear epitopes by IgA and IgG antibodies in COVID-19 patients with moderate and mild disease symptoms [34]. Using serum epitope repertoire analysis (SERA), dominant RBD epitope regions and motifs associated with disease symptomatology were identified in SARS-CoV-2 and were reactive with other coronaviruses but with a reduced antibody response in mutant SARS-CoV-2 strains [35]. Other studies have shown that neutralization of SARS-CoV-2 requires antibodies against conformational RBD epitopes [36]. These results provided evidence supporting that differences in antibody binding linear and conformational RBD epitopes may be associated with antibody isotype and disease symptomatology.

To address this possibility, in this study, we used high-throughput antibody binding epitope mapping using an RBD peptide array at amino acid resolution. This methodology has been previously validated for the characterization of the interactions between antibodies in COVID-19 patients at the S-ACE2 interface [28–30, 32–34, 37]. However, our study is novel by including IgA, IgM and IgG antibody isotypes and saliva and/or sera of different cohorts from healthy uninfected individuals and SARS-CoV-2-infected asymptomatic, recovered, nonsevere, and severe patients. For validation of identified candidate diagnostic, prognostic, and protective epitopes, sera from prevaccine and post-vaccine cohorts were used. Collectively, these results reveal novel epitopes for the development of new interventions for the diagnosis, prognosis, and prevention of COVID-19.

## Results

### Cohort-specific signatures in RBD epitope mapping

RBD epitope mapping was analyzed with a peptide microarray using the fluorescence intensity of immunoreactivity of IgA, IgM

**Table 1.** Identified reactive and candidate neutralizing protective epitopes/regions in the SARS-CoV-2 RBD protein

RBD epitopes/regions	Findings in COVID-19 patients	References
356-KRISN-360	IgG binding	[20]
	IgA (asymptomatic, nonsevere, severe) binding	This study
456-FRKS-460	IgG binding, candidate protective epitope	[20]
	IgA, IgM (nonsevere), IgG (asymptomatic) binding, candidate protective epitope (nonsevere)	This study
367-VLYNSASFSTFK-378	AI334/CR3022 antibody weak reaction	[9, 23]
	IgA (asymptomatic), IgG (recovered) binding	This study
388-LNDLCFTNVYAD-399	Low specificity to COVID-19 sera	[24]
	IgA low specificity to COVID-19 sera	This study
	IgM (nonsevere), IgG (asymptomatic) binding	
559-SNLKPFERDISTEY-573	Low specificity to COVID-19 sera	[25]
	Low specificity to COVID-19 sera	This study
	IgG (asymptomatic)	
	559-SNLKPFERD-567 binding	
573-YQAGSTPCNGVEGFN-587	Low specificity to COVID-19 sera	[25]
	Low specificity to COVID-19 sera	This study
343-NATRFASVYAWNRKR-357	IgA binding	[26]
	IgA, IgM (nonsevere), IgG (recovered) binding	This study
415-TGKIADYNYKLPDDF-429	IgA binding	[26]
	IgA (asymptomatic) binding	This study
449-YNYLYRFLRKS NLKP-463	IgA binding	[26]
	IgA, IgM (nonsevere), IgG (asymptomatic) binding	This study
369-YNSASFSTFKCYGVS-383	IgG binding	[26]
	IgG (recovered) binding	This study
364-DYSVLYNSASFSTF-377	IgA (asymptomatic) distinctive reactive epitope	This study
422-NYKLPDDFTGCVIAWNSNNL-441	IgA (asymptomatic) distinctive reactive immunodominant epitope	This study
488-NCYF-491	IgA (severe) distinctive reactive immunodominant epitope	This study
497-GFQPTNGVG-505	IgA (recovered) distinctive reactive immunodominant epitope	This study
510-VVLSFELLH-519	IgA (asymptomatic) distinctive reactive epitope	This study
319-RVQPTESIV-327	IgM (nonsevere) distinctive reactive epitope	This study
345-TRFASVYAWNRKR-357	IgM (nonsevere) distinctive reactive epitope	This study
388-LNDLCFTNVYADSFV-402	IgM (nonsevere) distinctive reactive epitope	This study
512-VLSFELLHAPATV-524	IgM (asymptomatic) distinctive reactive epitope	This study
525-CGPKKSTNLVKNK-537	IgM (nonsevere) distinctive reactive epitope	This study
347-FASVYAWNRKRI-358	IgG (recovered) distinctive reactive epitope	This study
363-ADYSVLYNSASFSTFKCY-380	IgG (recovered) distinctive reactive immunodominant epitope	This study
390-DLCFTN-395	IgG (asymptomatic) distinctive reactive epitope	This study
508-YRVVV-512	IgG (nonsevere) distinctive reactive epitope	This study
455-LFRKS NLKPFERD-467	IgG (asymptomatic) distinctive reactive and candidate protective epitope	This study
491-FPLQSYGF-498	IgG (asymptomatic) distinctive reactive and candidate protective epitope	This study
492-PLQSYGFQPTNGVG-505	IgA (recovered) candidate protective epitope	This study
446-GGNYNLYRFLRKS NL-461	IgA, IgM (nonsevere) distinctive reactive immunodominant and candidate protective epitope	This study
488-NCYFPLQSY-496	IgA (severe) candidate protective epitope	This study
332-ITNLCPFGEV-341	IgG (nonsevere) candidate prognostic epitope	This study
352-AWNRKRI-358	IgG (recovered) candidate prognostic epitope	This study
395-VYADSFVIRGDEV-407	IgG (nonsevere) candidate prognostic epitope	This study
524-VCGPKKSTNLVKN-536	IgG (severe) candidate prognostic epitope	This study



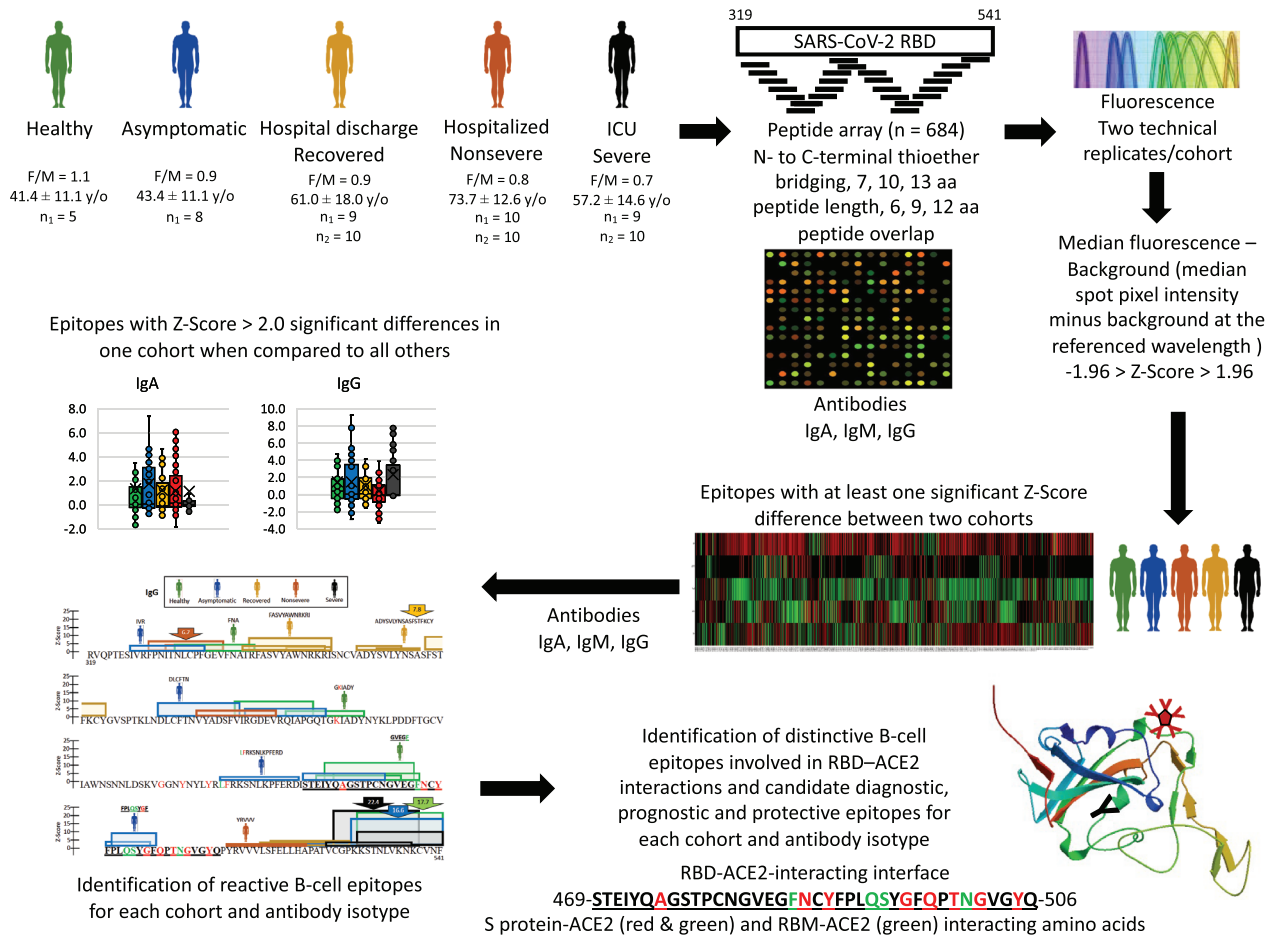


**Figure 1.** Experimental design for the identification of reactive RBD epitopes. Sera from 5 cohorts of healthy uninfected individuals and asymptomatic, recovered, nonsevere, and severe COVID-19 patients were used for linear epitope mapping of the SARS-CoV-2 RBD protein by antibody IgA, IgM, and IgG isotypes using a peptide microarray. The study included prevaccine cohorts of healthy, asymptomatic, nonsevere (hospitalized), recovered (hospital discharge), and severe (ICU) individuals, and additional sera from individuals not included in the RBD proteome microarray in cohorts of healthy, asymptomatic, nonsevere (hospitalized), recovered (hospital discharge), and severe (ICU) individuals were used for the characterization by ELISA of candidate diagnostic, prognostic and protective epitopes. The female to male (F/M) ratio and the age (average ± S.D. years-old; y/o) was calculated for all individuals included in the study. For RBD proteome microarray, sera from individuals in each cohort were pooled for analysis (n = 5–10 sera/pool and 1–2 pools/cohort (n<sub>1</sub>, pool 1; n<sub>2</sub>, pool 2)). Fluorescence Z-Score was used to identify reactive and distinctive B-cell epitopes involved in RBD-human ACE2 interactions and candidate diagnostic, prognostic, and protective epitopes for each cohort and antibody isotype.

and IgG antibody isotypes in healthy uninfected individuals and SARS-CoV-2-infected asymptomatic, recovered, nonsevere, and severe COVID-19 patients (Fig. 1 and Figs. S1 and S2). First, reactive epitopes with at least one significant Z-Score difference between two cohorts were identified (Fig. 2A). The results showed the presence of highly reactive epitopes associated with antibody isotype and cohort. Then, the analysis was focused on reactive epitopes with Z-Score > 2 and significant differences in one cohort when compared to all others (Fig. 2B and Figs. S1 and S2). The lowest and highest Z-Scores were obtained for IgM and IgG antibodies, respectively (Fig. 2B). A tendency toward lower Z-Scores was observed in sera from severe patients for IgA and IgM antibodies, but significant differences were found in nonsevere patients when compared to all others and in severe when compared to nonsevere patients (Fig. 2B). The mapped peptide sequences again showed the presence of highly reactive

epitopes associated with antibody isotype and cohort (Figs. S1 and S2). As previously reported for IgM and IgG antibodies [37], here, we found that RBD binding epitopes differ across IgA, IgM, and IgG antibodies (Fig. 2A and Figs. S1 and S2). The analysis of antibody isotype-distinctive reactive epitopes showed cohort-specific signatures with all IgM reactive epitopes also recognized by IgA and/or IgG antibodies (Fig. 2C). One reactive epitope was recognized only by IgG antibodies in sera from recovered patients. Twelve epitopes were only reactive to IgA antibodies by sera from different cohorts except healthy individuals.

Neutralizing anti-S RBD IgG antibodies were present in all cohorts (S-ACE2 inhibition, 33% to 93%) except for healthy uninfected individuals who were all negative (S-ACE2 inhibition, –0.4% to 4.3%) (Fig. 3A). A significant positive correlation was observed between antibody levels and S-ACE2 inhibition

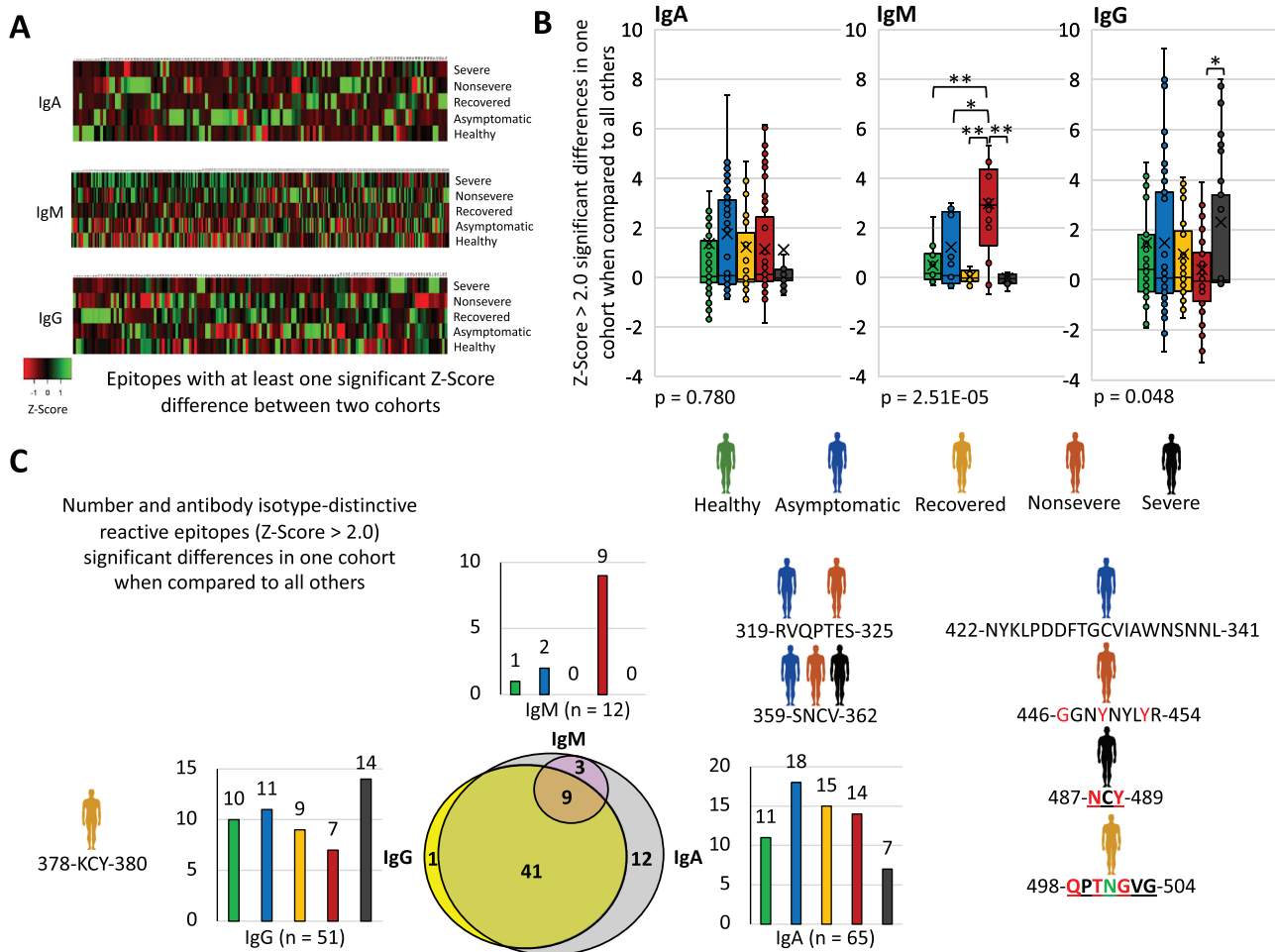


**Figure 2.** RBD epitope mapping. (A) Heatmap of the IgA-, IgM-, and IgG-reactive epitopes with at least one significant Z-Score difference between the two cohorts. (B) Distribution of reactive epitopes with Z-Score > 2 and significant differences in one cohort when compared to all others. The Z-Scores were compared between cohorts for each antibody isotype by one-way ANOVA (*p*-values included at the bottom of the graphs) followed by post hoc Bonferroni and Holm multiple comparisons (*\*p* < 0.05, *\*\*p* < 0.01). (C) Number and antibody isotype-distinctive reactive epitopes with Z-Score > 2 and significant differences in one cohort when compared to all others. Bold underlined letters correspond to the RND-ACE2-interacting interface and S protein-ACE2 (red & green) and RBM-ACE2 (green) interacting amino acids.

(Fig. 3A). Based on these results, discrimination with the healthy control cohort was performed by eliminating the RBD epitopes also recognized by sera from healthy individuals. Immunoreactive epitopes and regions were then identified for each antibody isotype and cohort with distinctive reactive immunodominant epitopes and regions (Fig. 3B and Table 1). For IgA antibodies, distinctive immunoreactive epitopes or regions were identified in all COVID-19 cohorts. However, distinctive epitopes or regions immunoreactive to IgM (identified in asymptomatic and nonsevere cohorts) and IgG (identified in asymptomatic, recovered, and nonsevere cohorts) were not identified with sera from severe patients. Nevertheless, the highest Z-Score values corresponded to IgA (Z-Score = 18.5) and IgG (Z-Score = 22.4) antibody isotypes in the severe cohort (Fig. 3B).

For the analysis of predicted neutralizing epitopes and regions recognized by different cohorts and antibody isotypes, antibody-RBD interactions were focused on pep-

tides located on the RBD-ACE2 interacting interface (469-STEIYQAGSTPCNGVEGFNCYFPLQSYGFQPTNGVGYQ-506) and S/RBD-human ACE2 interacting amino acids (Fig. 4 and Table 1). The results showed the presence of IgG isotype-predicted neutralizing epitopes or regions only in asymptomatic individuals. The distinctive IgA isotype epitopes or regions were identified in recovered, nonsevere, and severe cohorts. In sera from nonsevere patients, the predicted IgA neutralizing region was also reactive to IgM antibodies. These results provided a cohort and antibody isotype-specific signature for predicted neutralizing epitopes and regions.

To provide additional support for predicted neutralizing epitopes, serum and saliva collected from two asymptomatic cases with different spike-ACE2 inhibition (case 96, 41% and 40% inhibition and case 100, 0% and 89% inhibition in saliva and serum samples, respectively; Fig. 3) were used for RBD epitope mapping of IgA, IgM, and IgG antibodies. As expected,

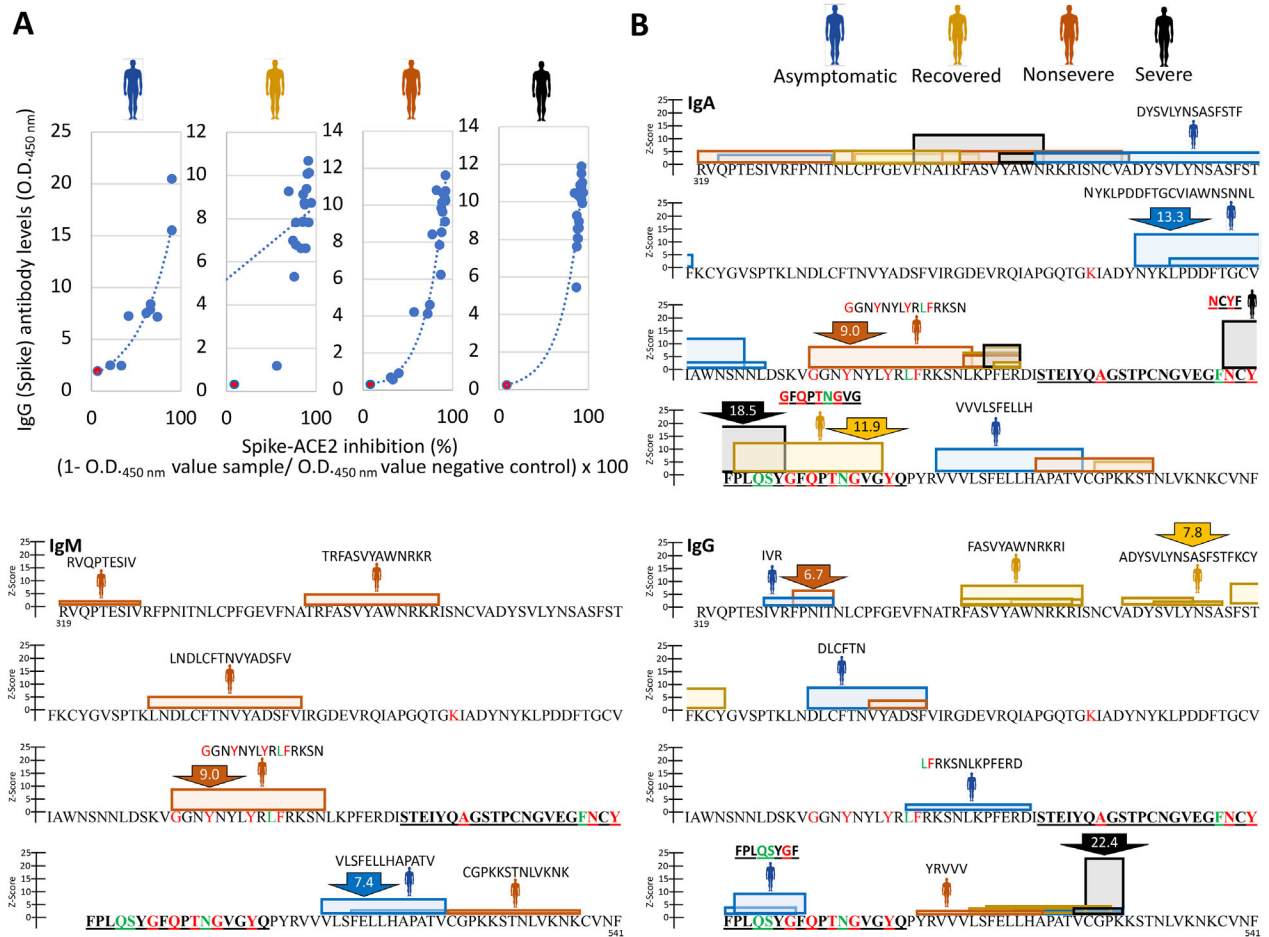


**Figure 3.** Immunoreactive RBD regions identified by sera from SARS-CoV-2-infected individuals. (A) Neutralizing anti-S IgG antibodies and Spearman's Rho correlation with S-ACE2 inhibition in asymptomatic ( $r_s = 0.8, p$  (2-tailed) = 0.002), recovered ( $r_s = 0.6, p$  (2-tailed) = 0.01), nonsevere ( $r_s = 0.9, p$  (2-tailed) < 0.00001), and severe ( $r_s = 0.7, p$  (2-tailed) = 0.0006) cohorts. Red spots correspond to negative sera (cutoff value, 30% S-ACE2 inhibition). Healthy uninfected individuals were all negative. (B) Mapping of RBD immunoreactive epitopes and regions to IgA, IgM, and IgG antibodies after discrimination with the healthy control cohort. Reactive distinctive and immunodominant (highest Z-Score, arrows) epitopes are shown. Bold underlined letters correspond to the RND-ACE2-interacting interface and S protein-ACE2 (red & green) and RBM-ACE2 (green) interacting amino acids.

differences in predicted neutralizing epitopes were not observed in serum samples between cases 96 and 100, where both showed Spike-ACE2 inhibition (Fig. 3). However, the results corroborated the predicted 455-LFRKSNLKPFERD-467 neutralizing epitope (Fig. 4 and Table 1) with saliva IgA antibodies in case 96 with Spike-ACE2 inhibition (Fig. 3).

### Translational medicine on diagnostic (asymptomatic cases) and prognostic (disease risks) markers

Our study approached the first RBD epitope mapping by IgA, IgM, and IgG antibody isotypes in sera from healthy uninfected individuals and SARS-CoV-2-infected asymptomatic, recovered, nonsevere, and severe patients. The study corroborated previous results and provided new findings on the antibody isotype and COVID-19 disease symptomatology signature of immunoreactive and predicted neutralizing RBD B-cell epitopes and regions

(Table 1). Herein, we addressed the implications of these results for translational medicine through the identification of reactive epitopes for the development of potential diagnostic (focused on asymptomatic cases), prognostic (disease risks) and preventive interventions.

### Candidate diagnostic epitopes for asymptomatic COVID-19 cases

The corroborated predicted 455-LFRKSNLKPFERD-467 neutralizing epitope (Fig. 4 and Table 1) with saliva IgA antibodies in case 96 with Spike-ACE2 inhibition (Fig. 3) was selected for the validation study using sera from all prevaccine and postvaccine cohorts (Fig. 5A and B) and paired serum-saliva from asymptomatic cases (Fig. 5C).

In prevaccine cohorts, the results showed significantly higher IgA antibody titers in asymptomatic individuals than in healthy

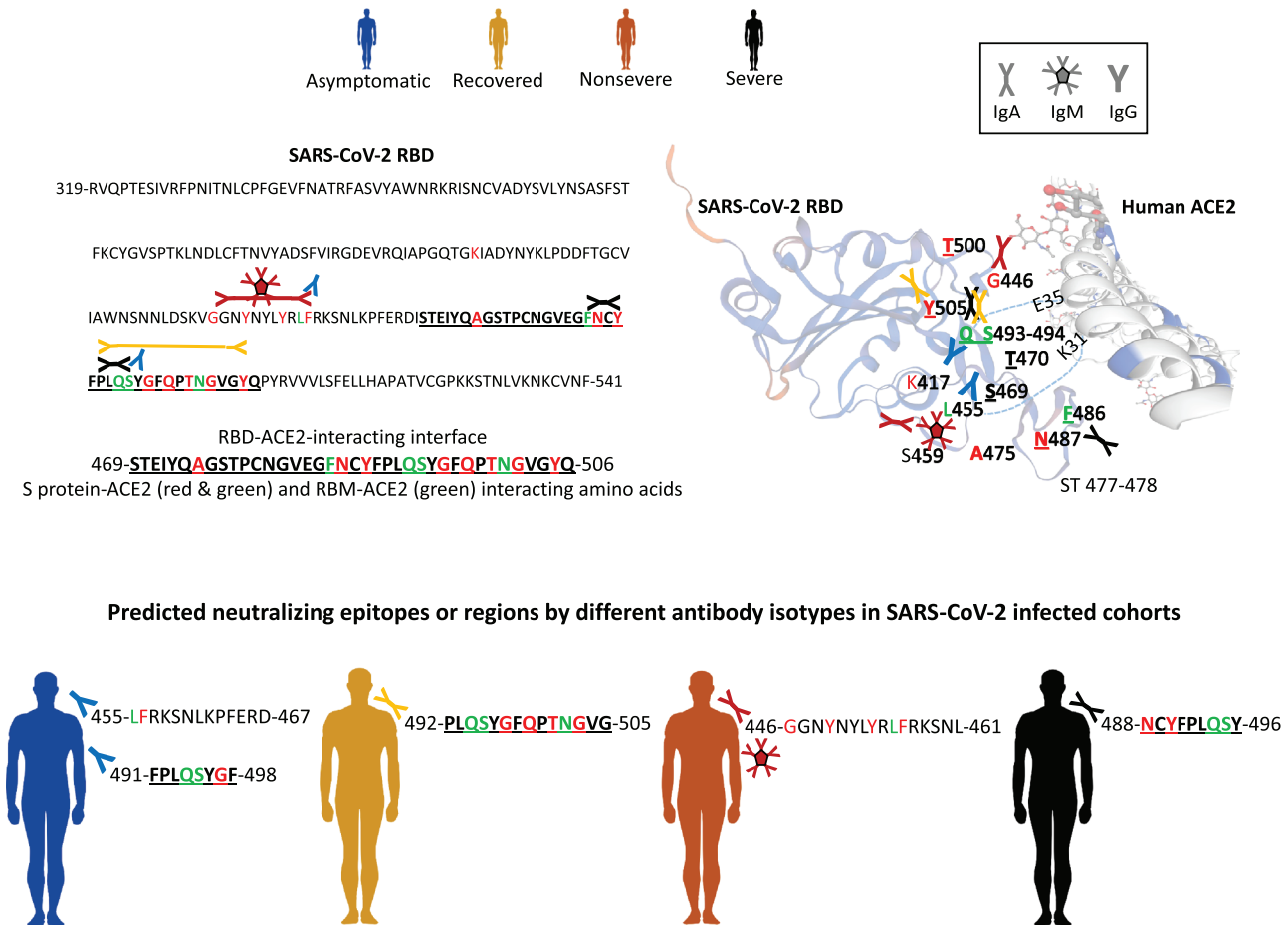


**Figure 4.** Predicted neutralizing epitopes and regions recognized by sera from SARS-CoV-2-infected cohorts. The analysis was focused on peptides located on the SARS-CoV-2 RBD-ACE2 interacting interface and S/RBD-human ACE2 interacting amino acids to identify the predicted neutralizing epitopes and regions recognized by different cohorts and antibody isotypes. The role of these epitopes and regions in the interaction between the SARS-CoV-2 RBD and human ACE2 was modeled based on target-template alignment using ProMod3 in the Swiss model.

controls ( $p < 0.01$ ; Fig. 5A). Additionally, IgA antibody titers in asymptomatic individuals were also higher than those in recovered, nonsevere, and severe patients ( $p < 0.04$ ; Fig. 5A). To reproduce the conditions after vaccination, sera from postvaccine cohorts were analyzed for IgA antibody response (Fig. 5B). Due to individual-to-individual variations, the results did not show differences in IgA antibody titers in postvaccine cohorts ( $p > 0.05$ ; Fig. 5B), thus suggesting that this epitope is not a good candidate for diagnosis in vaccinated individuals. Using serum and saliva collected from two asymptomatic cases with different spike-ACE2 inhibition described above (Fig. S3), the results showed recognition of the candidate diagnostic neutralizing epitope by serum and saliva IgA and IgG antibodies with higher titers for IgA antibodies (Fig. 5C).

These results confirmed the diagnostic capacity of the 455-LFRKSNLKPFFERD-467 neutralizing epitope for the detection of asymptomatic cases with IgA antibodies in prevaccine cohorts. In individuals vaccinated but with severe (ICU patients) symptomatology, IgG antibody levels against this epitope may have a prognostic capacity at least in some individuals.

### Candidate prognostic epitopes associated with COVID-19 disease risks

The results of pairwise comparisons of epitope mapping between different cohorts could be further explored to identify disease prognostic epitopes. For example, in some cases, hospitalized non-severe patients could progress to disease recovery (hospital discharge) or severity (ICU). Therefore, the identification of reactive epitopes with Z-Score significantly different between recovery-nonsevere and recovery-severe cohorts may be used as a prognostic biomarker at hospitalization. In our study, the results showed that some IgG-reactive epitopes with significant Z-Score differences produce an immunoreactive profile that may be used to evaluate the risk of hospitalized patients developing severe symptoms (Fig. 6A and Table 1).

The peptides with selected disease prognostic epitopes 395-VYADSFVIRGDEV-407-C-KLH, 332-ITNLCPFGEV-342-C-KLH, 352-AWNRKRI-358-C-KLH, and 524-VCGPKKSTNIVKN-536-KLH were characterized by ELISA using sera from individuals in different prevaccine cohorts (Fig. 6A). The results corroborated the



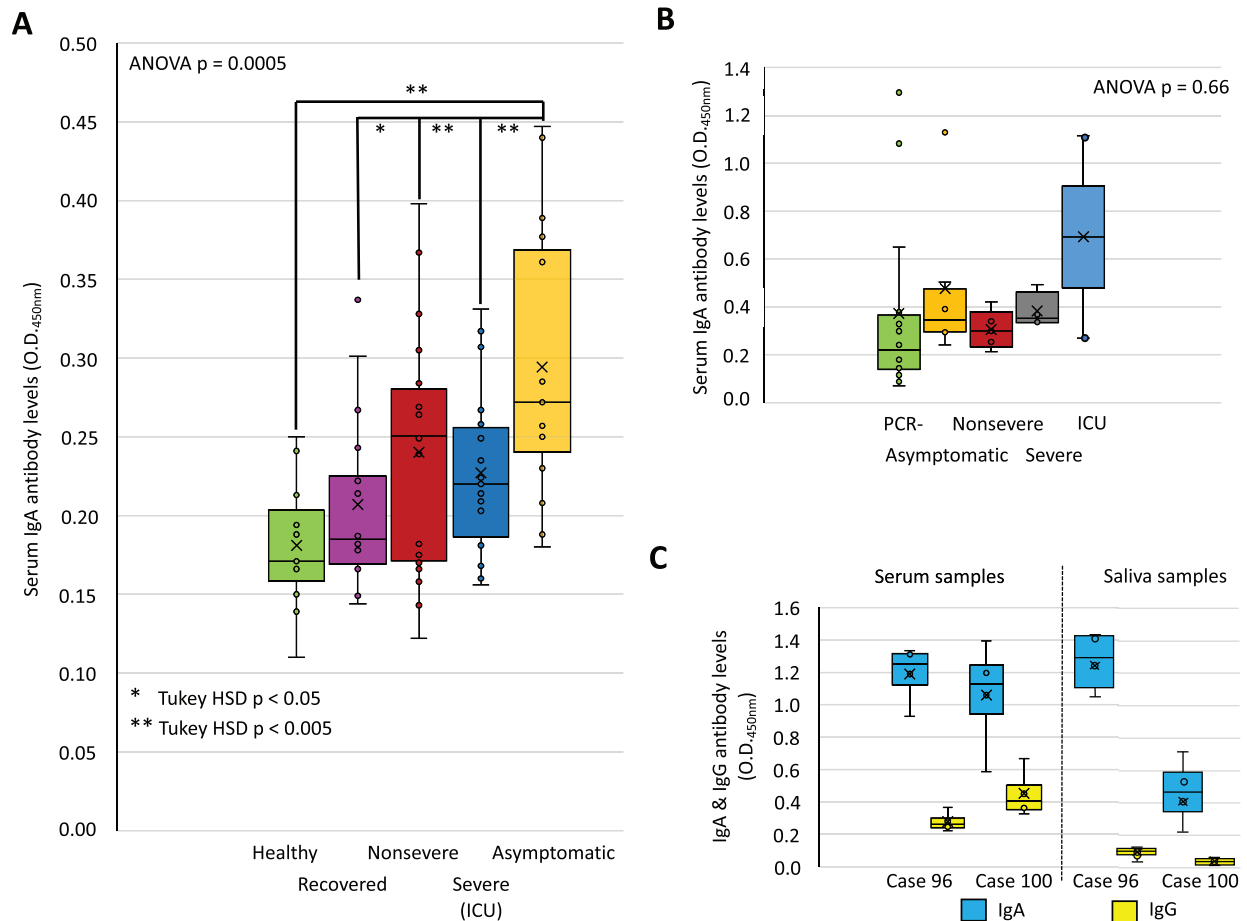


**Figure 5.** Predicted disease diagnostic epitope. (A) The 455-LFRKSNLKPFFERD-467 neutralizing epitope identified as a candidate diagnostic epitope was used for ELISA testing for IgA antibody levels in sera from individuals not included in the RBD proteome microarray in prevaccine cohorts of healthy ( $n = 11$ ), asymptomatic ( $n = 15$ ), nonsevere (hospitalized;  $n = 18$ ), recovered (hospital discharge;  $n = 17$ ), and severe (ICU;  $n = 18$ ) individuals. (B) Sera from postvaccine cohorts of PCR- ( $n = 14$ ) and PCR+ asymptomatic ( $n = 6$ ), nonsevere ( $n = 5$ ), severe ( $n = 5$ ), and ICU ( $n = 2$ ) individuals were analyzed for IgA antibodies. Antibody levels (O.D. 450 nm) were compared between groups by one-way ANOVA ( $p < 0.05$ ) followed by post hoc Tukey's HSD (\* $p < 0.05$ , \*\* $p < 0.005$ ). (C) An ELISA against the candidate diagnostic epitope was conducted using paired serum–saliva samples from asymptomatic cases 96 and 100 (4 replicates for each sample). On each graph, values (“circles”), mean (“x”), and median (“horizontal line”) are shown.

prognostic capacity of selected epitopes and suggested their use for the development of ELISA tests with prognostic capacity in hospitalized patients (Fig. 6B).

After vaccination, the IgG antibody response was only significantly higher in ICU patients when compared to all cohorts ( $p < 0.05$ ; Fig. 4). These results support the prognostic capacity of this epitope for severe symptomatology in vaccinated individuals. Additionally, three cases with 1–6 months after being detected positive for SARS-CoV-2 RT–PCR and with negative RT–PCR for SARS-CoV-2 when sampled were included to evaluate possible disease risks by ELISA (Fig. 4). These cases showed serum levels of ferritin and D-dimer prognostic biomarkers of COVID-19 disease severity below the established cutoff values (ferritin, 270–714 ng/ml; D-dimer, 1300–2100 ng/ml) [38, 39], suggesting low disease risks. These results were confirmed by all proposed prognostic epitopes in all three cases (Fig. 5), thus providing additional support for considering these peptides for developing prognostic ELISA tests.

### Translational medicine on vaccine (quantum vaccinomics) applications: Candidate protective epitopes

Recent results using RBD epitope mapping with antibodies from COVID-19 patients and healthy individuals immunized with the Pfizer-BioNTech COVID-19 mRNA vaccine (<https://www.cdc.gov/coronavirus/2019-ncov/vaccines/different-vaccines/Pfizer-BioNTech.html>) [40] identified epitopes recognized by both cohorts (e.g., 449-YNLYRFLFRKSNLKP-463) or by vaccinated individuals only (e.g., 363-ADYSVLYNSASFSTFKCY-380 and 332-ITNLCPFGEV-341) and present in regions identified in our study (Table 1).

Based on the results obtained in our study, we proposed a quantum vaccinomics approach to vaccine design for the control of COVID-19 by combining selected identified RBD protective epitopes and regions (Fig. 4, Table 1). For example, the RBD epitope 456-FRKS-460 was identified as an IgA,

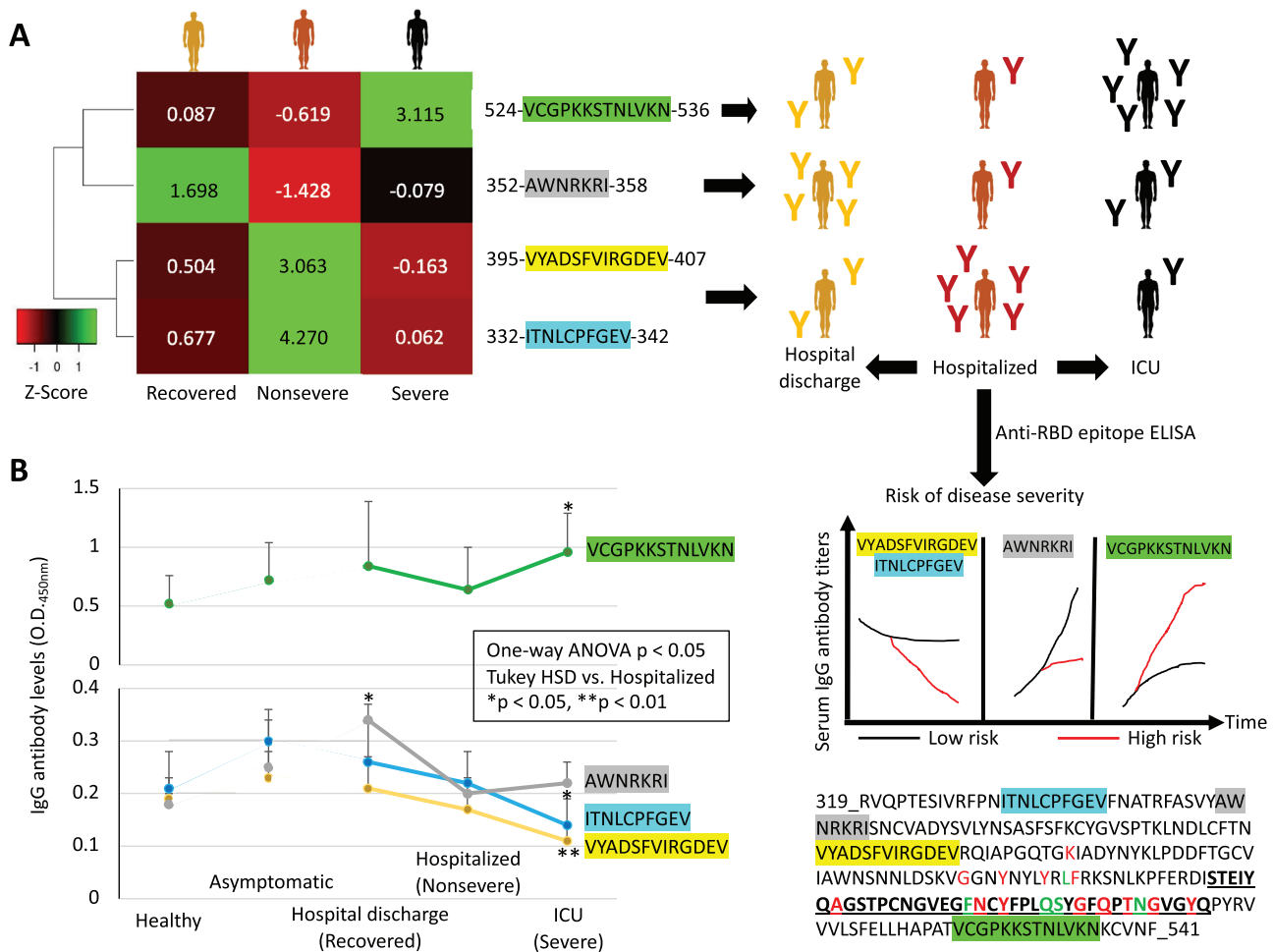


**Figure 6.** Predicted disease prognostic epitopes. (A) Pairwise comparison of Z Score significant differences between IgG-reactive recovery-nonsevere and recovery-severe cohorts. Cohorts of nonsevere (hospitalized;  $n = 20$ ), recovered (hospital discharge;  $n = 19$ ) and severe (ICU;  $n = 19$ ) individuals were included in the analysis. Z-Score values and the reactive epitopes are shown in the heatmap with Euclidean complete linkage. The position of the identified epitopes on the SARS-CoV-2 RBD-ACE2 interacting interface is highlighted with different colors. The immunoreactive profile of the different epitopes was used to predict the risk of hospitalized patients developing severe symptoms. Bold underlined letters correspond to the RND-ACE2-interacting interface and S protein-ACE2 (red & green) and RBM-ACE2 (green) interacting amino acids. (B) The peptides identified as candidate prognostic epitopes were used for ELISA tests using sera from individuals not included in the RBD proteome microarray in cohorts of healthy ( $n = 7$ ), asymptomatic ( $n = 7$ ), nonsevere (hospitalized;  $n = 8$ ), recovered (hospital discharge;  $n = 8$ ) and severe (ICU;  $n = 8$ ) individuals. Antibody levels (O.D. 450 nm; average + S.D.) were compared between nonsevere (hospitalized), recovered (hospital discharge) and severe (ICU) by one-way ANOVA ( $p < 0.05$ ) followed by post hoc Tukey's HSD ( $*p < 0.05$ ,  $**p < 0.01$  vs. hospitalized nonsevere).

IgM and IgG candidate protective epitope in previous and our studies (Table 1). In our study, the RBD regions containing the 456-FRKS<sub>N</sub>-460 protective epitope, 455-LFRKSNLKPFRD-467, and 446-GGNYNLYR<sub>L</sub>FRKSNL-461, were identified as candidate protective peptides using sera from asymptomatic and nonsevere SARS-CoV-2-infected individuals (Fig. 4 and Table 1). The epitope 492-PLQSY-496 was identified in our study in 491-FPLQSYGF-498, 492-PLQSYGFQPTNGVG-505 and 488-NCYFPLQSY-496 predicted candidate protective regions (Fig. 3 and Table 1). Other reactive epitopes identified in our study (i.e., 347-FASVYAWNRKRI-358, 363-ADYSVLYNSASFSTFKCY-380, and 510-VVLSFELLH-519) have been predicted as immunogenic epitopes for vaccine design [41, 42].

Considering the results of the RBD epitope mapping reported here and previous results with tick vaccine antigens [43, 44], we proposed the candidate SARS-CoV-2 protective chimeric antigen MKLLE-487-NCYFPLQSYGFQPTNGVG-504-GGGGS-446-GGNYNLYR<sub>L</sub>FRKSNLKPFRD-467. The chimeric antigen contains epitopes identified before as reactive in Pfizer-BioNTech vaccinated individuals (449-YNLYR<sub>L</sub>FRKSNLKP-463; [40]) and in the synthetic peptide RBD 446–480 shown to induce cross-reactive humoral neutralizing and cellular CD4 and CD8 responses in preclinical trials in mice (RBD 446–467; [45]).

First, IgA and IgG antibody responses against the candidate protective antigen were analyzed in sera from individuals in both pre- and postvaccine cohorts (Fig. 7A). The results showed

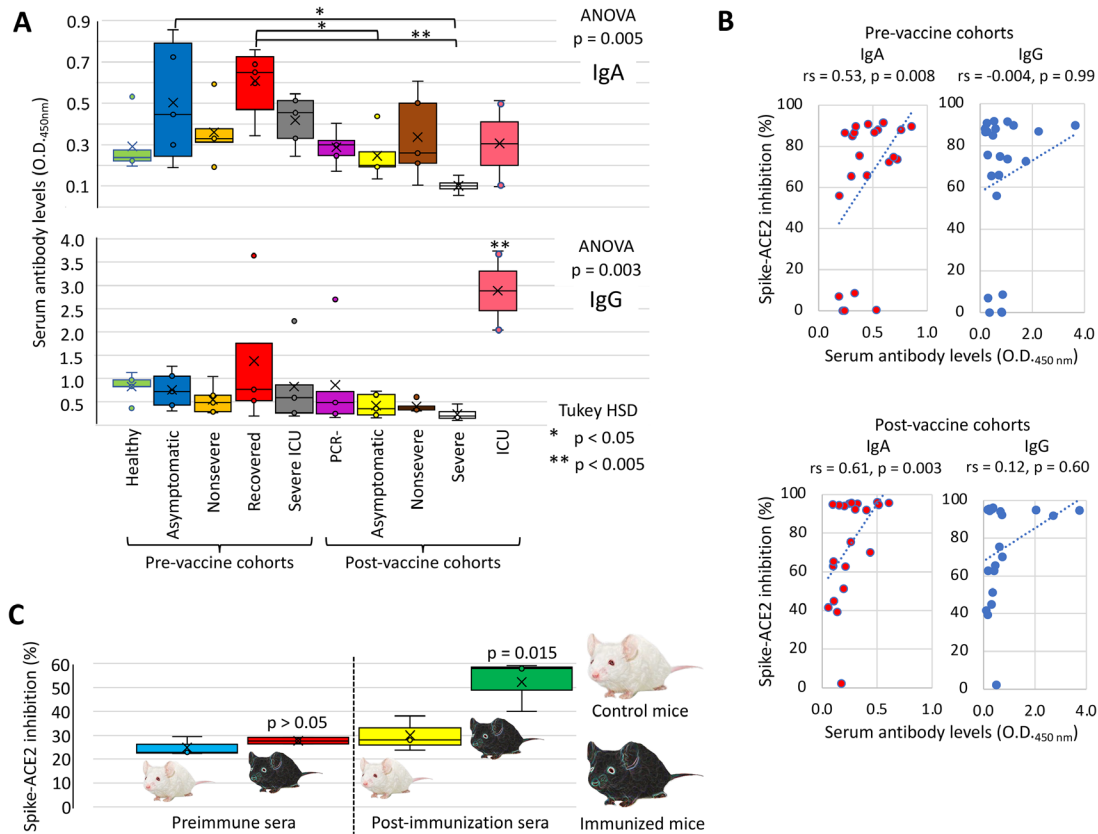


**Figure 7.** Candidate SARS-CoV-2 protective chimeric antigen. The analysis was conducted with the identified candidate SARS-CoV-2 protective chimeric antigen MKLLE-487-NCYFPLQSYGFQPTNGVG-504-GGGGS-446-GGNYNLYRLFRKSNLKPFRD-467. (A) Sera from prevaccine cohorts of healthy ( $n = 11$ ), asymptomatic ( $n = 15$ ), nonsevere (hospitalized;  $n = 18$ ), recovered (hospital discharge;  $n = 17$ ) and severe (ICU;  $n = 18$ ) individuals were analyzed together with postvaccine cohorts of PCR- ( $n = 6$ ) and PCR+ asymptomatic ( $n = 6$ ), nonsevere ( $n = 5$ ), severe ( $n = 5$ ) and ICU ( $n = 2$ ) individuals for IgA and IgG antibodies. Antibody levels (O.D. 450 nm) were compared between groups by one-way ANOVA ( $p < 0.05$ ) followed by post hoc Tukey's HSD (\* $p < 0.05$ , \*\* $p < 0.005$ ). (B) Serum IgA and IgG antibody levels against candidate protective chimeric antigen and Spearman's Rho correlation with S-ACE2 inhibition in prevaccine and postvaccine cohorts. (C) Mice were immunized with the candidate protective antigen or with PBS as a control. Sera collected before immunization (preimmune sera) or 3 days after the third immunization (postimmunization sera) were analyzed for neutralizing antibodies. The S-human ACE2 inhibition (%) was calculated as  $(1 - \text{O.D. 450 nm value sample} / \text{O.D. 450 nm value negative control}) \times 100$ , cutoff value 30% S-ACE2 inhibition and compared between control and immunized mice by Student's *t*-test with unequal variance ( $p < 0.05$ ).

the highest IgA antibody levels in prevaccine asymptomatic and recovered cohorts, while IgG antibody levels were significantly higher in postvaccine ICU individuals than in all other pre- and postvaccine cohorts (Fig. 7A). A significant positive correlation was observed between anti-candidate protective antigen IgA antibodies and neutralization of S-human RBD interactions in both pre- and postvaccine cohorts (Figure 7B). These results are associated with IgA binding to these epitopes identified in COVID-19 patients (Table 1). The anti-candidate protective antigen IgG antibodies and neutralization of S-human RBD interactions showed a tendency but not significant positive correlation in both pre- and postvaccine cohorts (Fig. 7B). The mouse model was used to evaluate the neutralization capacity of total antibodies in response to vaccination with the candidate protective antigen. Only mice immunized with the candidate protective antigen developed neutralizing antibodies for S-human RBD interactions (average  $\pm$  SD,  $52.4 \pm 10.7\%$  inhibition,  $p = 0.015$ ; Fig. 7C). These results support the protective capacity of the proposed chimeric antigen.

## Implications for the emergence and spread of SARS-CoV-2 Omicron variants of concern

Using the recently identified SARS-CoV-2 B.1.1.529 variant of concern Omicron [46], we identified amino acid changes present in our predicted diagnostic, prognostic, and protective epitopes (Fig. S6). Mutations were rare in predicted diagnostic and prognostic epitopes (only one for a single peptide on each diagnostic and prognostic epitopes; Fig. S6), suggesting the possibility of developing tests based on these peptides for the diagnostic and prognostic interventions of multiple SARS-CoV-2 genetic variants.

## Discussion

The characterization of the humoral antibody response to the SARS-CoV-2 S-RBD protein involved in virus–host interactions and infection is important to advance the development of

effective diagnostic, therapeutic and preventive interventions. Despite recent advances in these areas contributing to the control of the COVID-19 pandemic [47, 48], the challenge posed by new SARS-CoV-2 variants and other emerging coronaviruses requires research to better understand host–virus interactions and induced immunity [49–54]. Recent publications have provided information on the linear B-cell epitopes in the SARS-CoV-2 S protein, suggesting differences in antibody binding to linear RBD epitopes and regions that may be associated with antibody isotype and disease symptomatology [28–30, 32–34, 40]. In this study, we addressed this possibility through high-throughput antibody binding epitope mapping using an RBD peptide array at amino acid resolution.

Because asymptomatic COVID-19 cases are difficult to diagnose and constitute a risk for virus transmission [55, 56], surveillance of asymptomatic infected individuals contributes to the reduction of local disease outbreaks [57, 58]. Recent results have shown that the early neutralizing humoral response is mediated by IgA antibodies to SARS-CoV-2 [59]. In our study, the identified diagnostic capacity of the 455-LFRKSNLKPFRD-467 neutralizing epitope may be relevant for the detection of asymptomatic cases with IgA antibodies found in easy to collect oral, nasal and saliva samples [60]. Prognostic epitopes were also identified and validated in both pre- and postvaccine cohorts, thus providing new tools for the development of ELISA tests with prognostic capacity, particularly in hospitalized patients. The identification of candidate prognostic epitopes in the RBD-ACE2 interacting region (524-VCGPKKSTNIVKN-536) supports that neutralizing antibodies do not have to be in this region and may be conformationally hidden [61]. Additionally, these antibodies may be cross-reactive to other epitopes affecting disease severity [4].

The identification of protective epitopes in SARS-CoV-2 proteins, including the RBD, is necessary for vaccine development [62–65]. However, the use of RBD in vaccines has been challenging due to its limited immunogenicity, likely associated with its low molecular size and polymer structure [65]. To address these challenges, vaccine antigen design has included multiple copies of RBD on particles for the control of SARS-CoV-2 and other betacoronaviruses, such as Middle East respiratory syndrome coronavirus (MERS-CoV) and SARS-CoV [66]. An alternative approach to overcome RBD limitations in vaccine development is the combination of protective epitopes to improve the antibody response against immunization [41, 42, 67].

Quantum vaccinomics is a platform proposed for the identification and combination of antigen protective epitopes, the immunological quantum, for vaccine development [68, 69]. This platform focuses on the characterization of host–pathogen molecular interactions using a systems biology approach for the analysis of omics datasets [70]. A proposed pipeline for quantum vaccinomics is based on the characterization of the cell interactome and regulome in vector–host–pathogen interactions and the identification of protective epitopes in protein interacting domains for the design and production of chimeric vaccine antigens [68, 69, 71, 72]. This platform also provides the possibility of including other biomolecules, such as glycan alpha-gal (Gal $\alpha$ 1-

3Gal $\beta$ 1-(3)4GlcNAc-R)-based protein posttranslational modifications, to improve protective immunity against SARS-CoV-2 and other pathogens [73–76]. Taken together, the results of this study suggest the possibility of translating the findings of B-cell linear epitope mapping for quantum vaccinomics in designing vaccines with increased antibody and CD4<sup>+</sup>/CD8<sup>+</sup> T-cell responses for the control of SARS-CoV-2 genetic variants [28, 41, 42, 46, 77].

The antibody response to candidate protective chimeric antigen showed higher IgA antibody levels and neutralizing capacity in prevaccine asymptomatic and recovered individuals, which correlates with higher protective capacity in these cohorts infected with SARS-CoV-2. However, the lack of a significant positive correlation between anti-candidate protective antigen IgG antibodies and neutralization of S-human RBD interactions together with the highest IgG antibody levels in ICU patients suggested that the designed protective chimeric antigen may be more effective in eliciting the early neutralizing antibody response to SARS-CoV-2 [59]. The results in the mouse model support the possibility of eliciting a protective response to SARS-CoV-2 using this antigen.

Recently, the RLFKSNLKPFRDISTEI peptide was identified as highly reactive to mouse monoclonal antibodies with neutralizing capacity [78] and contains epitopes that were validated in our study as candidate diagnostic and protective epitopes. The other peptide identified as reactive to monoclonal antibodies but with low neutralizing capacity, VYADSFVIRGDEVRQIAPG [78], contains an epitope that was validated in our study as a candidate prognostic epitope. Deep mapping of mutations in the SARS-CoV-2 RBD affecting recognition by human plasma polyclonal antibodies identified F456 and E484 as the most important sites for mutations reducing virus neutralization [79]. In our study, F456 but not E484 was present in identified reactive and candidate neutralizing protective epitopes (Table 1). These findings support that the combination of results from different epitope mapping platforms provides information to advance the development of more effective interventions for disease diagnosis and control.

Although the methodological approach employed in this study has been validated, the limitations of our study include (a) the inclusion of linear epitopes only, although with a high coverage and throughput antibody binding epitope mapping, (b) not including in the array other SARS-CoV-2 variants that are arising with risks for transmission and disease worldwide and which should be included in future studies with selected peptide arrays based on this and other studies, (c) the use of sera from adult but not younger COVID-19 patients who may have differences in humoral immune response, and (d) the use of pooled sera, which was necessary to facilitate the analysis of IgA, IgM, and IgG antibody isotypes in SARS-CoV-2-infected cohorts with different symptomatology to address some of the limitations of previous studies. Additionally, as in other studies, we do not know how long after infection the blood samples were drawn for analysis, a fact that affects antibody response and class switching. Nevertheless, the results were validated in pre- and postvaccine cohorts for candidate diagnostic, prognostic, and protective epitopes.

In conclusion, the results of this study support that antibody recognition of linear B-cell epitopes in the SARS-CoV-2 RBD



protein is associated with antibody isotype and disease symptomatology. The identification of distinctive reactive immunodominant and candidate protective epitopes in SARS-CoV-2-infected individuals from asymptomatic to severe cases is novel. In agreement with previous reports, these results support that the humoral immune response contributes to recovery in most infected people in many cases without medical interventions. The findings in asymptomatic individuals suggest a role for anti-RBD antibodies in the protective response against SARS-CoV-2. The possibility of translating the results of our study into diagnostic interventions for the early diagnosis of asymptomatic individuals and prognosis of disease severity provides new tools for COVID-19 surveillance and evaluation of risks in hospitalized patients. Antibody-based therapeutics hold great promise in the treatment and prevention of multiple infectious diseases. Additionally, these results may contribute to the development of new vaccines for the control of COVID-19 and other coronavirus-related diseases using a quantum vaccinomics approach.

## Materials and methods

### Samples from healthy individuals and COVID-19 patients

The experimental design included prevaccine cohorts of healthy, asymptomatic, nonsevere (hospitalized), recovered (hospital discharge), and severe (ICU) individuals [2] (Figure 1). Additionally, sera from individuals not included in the RBD proteome microarray in cohorts of healthy, asymptomatic, nonsevere (hospitalized), recovered (hospital discharge), and severe (ICU) individuals [2] were used for the characterization by ELISA of candidate diagnostic, prognostic, and protective epitopes. This retrospective case-control study was conducted in patients suffering from COVID-19 and healthy controls sampled at the University General Hospital of Ciudad Real (HGUCR), Spain [2–4, 80, 81]. Blood samples from control healthy individuals were collected prior to the COVID-19 pandemic in April 2019. COVID-19 patients were confirmed as SARS-CoV-2-infected by IgG antibody titers or reverse transcriptase-PCR (RT-PCR) and sampled between March and May 2020 [2]. Clinical symptoms and laboratory determinations associated with COVID-19 were obtained from the patients' medical records to create the cohorts. Patients were hospitalized for developing a moderate-severe clinical condition with radiologically demonstrated pneumonia and failure in blood oxygen saturation. Patients with acute respiratory failure who needed mechanical ventilation support were admitted to a hospital ICU. The patients were discharged from the hospital due to the clinical and radiological improvement of pneumonia caused by SARS-CoV-2, along with the normalization of analytical parameters indicative of inflammation. For the validation of candidate diagnostic, prognostic and protective epitopes, sera from individuals vaccinated against COVID-19 were also included with vaccine administration, clinical symptoms, and laboratory

determinations associated with COVID-19 obtained from the patient's medical records to create cohorts of PCR-negative (PCR-) and PCR-positive (PCR+) asymptomatic, nonsevere, and severe individuals [4]. Data can be found in Urrea et al. [2] and Villar et al. [3, 4] and are summarized in Supplementary Table 1. Blood samples were drawn in a vacutainer tube without anticoagulant. The tube remained at rest for 15–30 min at room temperature (RT) for clotting. Subsequently, the tube was centrifuged at 1500 x g for 10 min at RT to remove the clot and obtain serum. Serum samples were heat-inactivated for 30 min at 56°C and stored at –20°C until used for analysis. Additionally, saliva-serum paired samples were collected from randomly selected asymptomatic cases, heat-inactivated for 30 min at 56 °C and conserved at –20 °C until used for analysis. Written informed consent for participation was not required for this study in accordance with national legislation and institutional requirements. The use of samples and individual data was approved by the Ethical and Scientific Committees (University Hospital of Ciudad Real C-352 and SESCAM C-73).

### SARS-CoV-2 RBD proteome microarray

To produce the peptide RBD microarray (PEPPERPRINT GmbH, Heidelberg, Germany), the reference sequence of RBD was used from the original isolate of the SARS-CoV-2 Wuhan-Hu-1 coronavirus genome from the National Center for Biotechnology Information (NCBI) database (Accession No MN908947) [82]. Peptide RBD microarray (RBD elongated with neutral GSGSGSG linkers at the C- and N-terminus and translated into overlapping peptides, n = 684 printed in duplicate for a total of 1,368 spots), N- to C-terminal thioether bridging with 7, 10, 13 amino acids peptide length and 6, 9, 12 amino acids peptide overlap. The peptide microarrays were stored at 4°C until use.

### Antibody isotype binding to the RBD proteome microarray

Cohorts of healthy (n = 5), asymptomatic (n = 8), nonsevere (hospitalized; n = 20), recovered (hospital discharge; n = 19) and severe (ICU; n = 19) individuals [2] were included in the analysis (Figure 1). Sera from individuals in each cohort were pooled for analysis (n = 5–10 sera/pool and 1–2 pools/cohort; Figure 1). Saliva collected from two asymptomatic cases with different spike-ACE2 inhibition (case 96, 41% and 40% inhibition and case 100, 0% and 89% inhibition in saliva and serum samples, respectively) were also used for analysis. The peptide microarrays were assembled in an incubation tray and blocked with 1% (w/v) BSA in 1 × PBS 7.4 with 0.005% (v/v) Tween-20 (PBST) for 30 min at RT. After it was washed with PBST three times, the array was incubated with pooled sera of each cohort or individual serum/saliva samples overnight at 4°C. The next day, it was washed again, and the arrays were incubated with rabbit anti-human IgA

Cy5, goat anti-human IgM (Mu chain) DyLight 549 and IgG Fc cross-adsorbed goat anti-human DyLight 550 (Invitrogen) for 45 min at RT. The arrays were washed, disassembled from the tray, and dried by centrifugation for 2 min at 2000 rpm. The resulting array was scanned with a GenePix personal 4100a microarray scanner (Molecular Devices, San Jose, CA, USA). The median fluorescent signal intensity of each spot was extracted using MAPIX software (Molecular Devices). The median background signal was subtracted from the median spot signal intensity.

### Analysis of RBD protein microarray data

Data were analyzed following methods described by Wang et al. [28]. The intensity of the raw fluorescence signal corresponded to the median signal intensity subtracted by the median background intensity of each spot and then averaged across duplicate spots. The resulting signals were normalized with a Z-Score [83],  $Z\text{-Score} = (\text{intensity}_P - \text{mean intensity}_{P1...Pn}) / \text{SD}_{P1...Pn}$ , where P is any RBD peptide on the microarray, and P1...Pn represents the aggregate measure of all peptides. The heatmaps of antibody binding to the peptides were visualized using the Z-Score heatmapper (<http://www.heatmapper.ca/expression/>). The Z-Score was also compared between cohorts for each antibody isotype by one-way ANOVA followed by Tukey's honestly significant difference (HSD) post hoc test ( $p < 0.05$ ; [https://astatsa.com/OneWay\\_Anova\\_with\\_TukeyHSD/](https://astatsa.com/OneWay_Anova_with_TukeyHSD/)). Only epitopes with at least one significant Z-Score difference between two cohorts were used to build the heatmaps, and then the analysis was focused on the epitopes with Z-Score  $> 2.0$  and significant differences in one cohort when compared to all others. Immunoreactive epitopes and regions (overlapping epitopes with similar results) were identified for each antibody isotype and cohort. The RBD-human ACE2 (NM\_001371415.1) interacting interface (469-STEIYQAGSTPCNGVEGFNCYFPLQSYGFQPTNGVGYQ-506) and S-human ACE2 interacting amino acids (K417, G446, Y449, Y453, L455, F456, A475, F486, N487, Y489, Q493, G496, Q498, T500, N501, G502, Y505) containing the RBD-human ACE2 interacting amino acids (L455, F486, Q493, S494, N501) were obtained from previously published results [29, 84–86]. A model of RBD-human ACE2 interaction was built based on the target-template alignment using ProMod3 [87] on Swiss model (<https://swissmodel.expasy.org>).

### Neutralizing antibody test

The neutralization antibody test (cPass<sup>TM</sup> SARS-CoV-2 Neutralization Antibody Detection Kit, GenScript Biotech, Leiden, The Netherlands B.V.) was conducted in all serum samples included in the RBD epitope mapping (Figure 1) and in saliva-serum paired samples from two randomly selected asymptomatic cases, following the manufacturer's recommendations. Data for postvaccine cohorts were obtained from Villar et al. [4]. Antibody titers specific for the recognition of virus infection

based on IgG against SARS-CoV-2 Spike (EI 2606-9601G) protein were determined by ELISA (Euroimmun, Lubeck, Germany) as O.D. 450 nm values following the manufacturer's instructions [2]. Spearman's rho correlation analysis (<https://www.socscistatistics.com/tests/spearman/default2.aspx>) was conducted between serum anti-S IgG antibody levels or anti-candidate protective chimeric antigen IgA and IgG antibody levels (O.D. 450 nm) and S-human ACE2 inhibition (%) as  $(1 - \text{O.D. 450 nm value sample} / \text{O.D. 450 nm value negative control}) \times 100$ . Cutoff value, 30% S-ACE2 inhibition.

### Characterization of human IgA and IgG antibody responses to candidate diagnostic epitopes

A peptide was identified as a candidate diagnostic epitope for asymptomatic individuals. The peptide was synthesized as keyhole limpet hemocyanin (KLH)-conjugated 455-LFRKSNLKPFRD-467-C-KLH peptide (GenScript Biotech). The peptide was used for analysis of the human IgA antibody response by ELISA using sera from individuals not included in the RBD proteome microarray in prevaccine cohorts of healthy ( $n = 11$ ), asymptomatic ( $n = 15$ ), nonsevere (hospitalized;  $n = 18$ ), recovered (hospital discharge;  $n = 17$ ), and severe (ICU;  $n = 18$ ) individuals and paired serum-saliva samples from asymptomatic cases 96 and 100 (4 replicates for each sample) [2]. Sera from vaccinated against COVID-19 cohorts of PCR- ( $n = 14$ ) and PCR+ asymptomatic ( $n = 6$ ), nonsevere ( $n = 5$ ), and severe ( $n = 7$  including two cases in ICU) individuals [4] were also included in the analysis. For ELISA, high absorption capacity polystyrene microtiter plates were coated with 100 ng of synthetic peptide per well in carbonate-bicarbonate buffer (Sigma-Aldrich, St. Louis, MO, USA). After an overnight incubation at 4°C, coated plates were washed one time with 100  $\mu\text{l}$ /well PBS with 0.05% Tween 20 (PBST) (Sigma-Aldrich), blocked with 100  $\mu\text{l}$ /well of 3% skim milk in PBS (blocking solution) for 1 h at RT and then washed 3 times with 100  $\mu\text{l}$ /well of PBST. Human serum samples were diluted 1:100 and 1:10 (optimum 1:100 used for analysis) in blocking solution, and 100  $\mu\text{l}$ /well was added into the wells of antigen-coated plates and incubated for 1 h at 37°C. Plates were washed three times with PBST, and 100  $\mu\text{l}$ /well of goat anti-human IgA secondary antibody (Sigma-Aldrich) diluted 1:1000 v/v in blocking solution was added and incubated for 1 h at RT. Plates were washed three times with 100  $\mu\text{l}$ /well PBST, and 100  $\mu\text{l}$ /well 3,3',5,5'-tetramethylbenzidine TMB (Promega, Madison, WI, USA) was added and incubated for 15 min at RT. Finally, the reaction was stopped with 50  $\mu\text{l}$ /well of 2 N H<sub>2</sub>SO<sub>4</sub> and the O.D. was measured in a spectrophotometer at 450 nm. The average of two technical replicates per sample was used for analysis after background (coated wells incubated with PBS and secondary antibodies alone). Antibody levels (O.D.450 nm) were compared between groups by one-way ANOVA followed by post hoc Tukey's HSD and Bonferroni and Holms tests ( $p < 0.05$ ; [https://astatsa.com/OneWay\\_Anova\\_with\\_TukeyHSD/](https://astatsa.com/OneWay_Anova_with_TukeyHSD/)).

## Characterization of human IgG antibody response to candidate prognostic epitopes

The peptides identified as candidate prognostic epitopes were synthesized as KLH-conjugated peptides 395-VYADSFVIRGDEV-407-C-KLH, 332-ITNLCPFGEV-342-C-KLH, 352-AWNRKRI-358-C-KLH, and 524-VCGPKKSTNLVKN-536-KLH (GenScript Biotech). These peptides were used for analysis of the human IgG antibody response by ELISA tests using sera from individuals not included in the RBD proteome microarray in cohorts of healthy (n = 7), asymptomatic (n = 7), nonsevere (hospitalized; n = 8), recovered (hospital discharge; n = 8), and severe (ICU; n = 8) individuals [2]. Sera from vaccinated against COVID-19 cohorts of PCR- (n = 6) and PCR+ asymptomatic (n = 6), nonsevere (n = 5), and severe (n = 7 including two cases in ICU) individuals [4] were also included in the analysis. Additionally, three cases 1–6 months after being positive for SARS-CoV-2 RT-PCR and with negative RT-PCR and D-dimer and ferritin data at the sampling time were included to evaluate possible disease risks by ELISA. For ELISA, high absorption capacity polystyrene microtiter plates were coated with 100 ng of each synthetic peptide per well in carbonate-bicarbonate buffer (Sigma–Aldrich). After an overnight incubation at 4°C, coated plates were washed one time with 100 µl/well PBS with 0.05% Tween 20 (PBST) (Sigma–Aldrich), blocked with 100 µl/well of 3% skim milk in PBS (blocking solution) for 1 h at RT and then washed 3 times with 100 µl/well of PBST. Human serum samples were diluted 1:100 and 1:10 (optimum 1:100 used for analysis) in blocking solution, and 100 µl/well was added into the wells of antigen-coated plates and incubated for 1 h at 37°C. Plates were washed three times with PBST, and 100 µl/well goat anti-human immunoglobulin-peroxidase IgG (FC specific) or goat anti-human IgA secondary antibodies (Sigma–Aldrich) diluted 1:1000 v/v in blocking solution were added and incubated for 1 h at RT. Plates were washed three times with 100 µl/well PBST, and 100 µl/well 3,3',5,5'-tetramethylbenzidine TMB (Promega) was added and incubated for 15 min at RT. Finally, the reaction was stopped with 50 µl/well of 2 N H<sub>2</sub>SO<sub>4</sub> and the O.D. was measured in a spectrophotometer at 450 nm. The average of two technical replicates per sample was used for analysis after background (coated wells incubated with PBS and secondary antibodies alone). Antibody levels (O.D.450 nm) were compared between nonsevere (hospitalized), recovered (hospital discharge) and severe (ICU) by one-way ANOVA test followed by post hoc Tukey HSD (p < 0.05; [https://astatsa.com/OneWay\\_Anova\\_with\\_TukeyHSD/](https://astatsa.com/OneWay_Anova_with_TukeyHSD/)).

## Characterization of human IgA and IgG antibody responses to candidate protective epitopes

The candidate SARS-CoV-2 protective chimeric antigen with the N-terminal peptide MKLLE and linker sequence GGGGS, MKLLE-487-NCYFPLQSYGFQPTNGVG-504-GGGGS-446-GGNYNLYRLFRKSNLKPFRD-467, was chemically synthesized by GenScript Biotech with more than 95% purity. The peptide

was used for analysis of human IgA and IgG antibody responses by ELISA using sera from individuals not included in the RBD proteome microarray in cohorts of healthy (n = 11), asymptomatic (n = 15), nonsevere (hospitalized; n = 18), recovered (hospital discharge; n = 17) and severe (ICU; n = 18) individuals. The IgA and IgG antibody responses were also analyzed in conjunction with postvaccine cohorts of PCR- (n = 6) and PCR+ asymptomatic (n = 6), nonsevere (n = 5), and severe (n = 7, including two cases in the ICU) patients [4]. ELISA was conducted as described above for candidate diagnostic epitopes.

## Characterization of neutralizing antibodies in mice immunized with the candidate protective chimeric antigen

Three female BALB/c mice, 4–6 weeks old, were immunized intraperitoneally with 3 doses of 20 µl (1.25 µg/µl) of candidate protective chimeric antigen emulsified with Freund's complete adjuvant (first dose) and Freund's incomplete adjuvant (second and third doses) (Sigma–Aldrich) at 3-week intervals. The control group with 3 mice was immunized with PBS with the same adjuvants and serum obtained in a similar way. Blood was collected from each mouse from the tail before immunization and by cardiac puncture 3 days after the third immunization and centrifuged at 2000 x g for 10 min. Serum was recovered from each sample, and the pellet was discarded. Sera from immunized and control mice were analyzed for total neutralizing antibodies as described above for human samples using the neutralization antibody test (cPass™ SARS-CoV-2 Neutralization Antibody Detection Kit, GenScript Biotech). The S-human ACE2 inhibition (%) was calculated as (1- O.D. 450 nm value sample/O.D. 450 nm value negative control) x 100, cutoff value 30% S-ACE2 inhibition and compared between control and immunized mice by Student's t test with unequal variance (p < 0.05). Animal experimentation was approved by the Ethical Committee of IHMT and the DGAV-Direção General de Agricultura e Veterinária (Portugal; reference 0421/2022 from July 8th, 2022).

**Acknowledgments:** This study was supported by Ministerio de Ciencia e Innovación/Agencia Estatal de Investigación, Spain and EU-FEDER [Grant BIOGAL PID2020-116761GB-I00]. M.C. was funded by the Ministerio de Ciencia, Innovación y Universidades, Spain, grant IJC2020-042710-I. RV-R was funded by Universidad de Castilla-La Mancha (UCLM), Spain and the European Social Fund (ESF) [grant 2022-PRED-20675].

**Author contributions:** J.F., M.C., C.G., and J.J.C. conceived and designed the study; M.C., J.M.U., F.J.R., E.F.-C., R.V.-R., I.G.F., S.M.S., and A.D. performed the experiments; M.C., J.V., and J.F.

analyzed the data; and J.F. and M.C. wrote the paper. All authors read and approved the final manuscript.

**Conflict of interest:** The authors declare no financial or commercial conflict of interest.

**Ethics approval:** Written informed consent for participation was not required for this study in accordance with national legislation and institutional requirements. The use of samples and individual data was approved by the Ethical and Scientific Committees (University Hospital of Ciudad Real C-352 and SESCAM C-73). Animal experimentation was approved by the Ethical Committee of IHMT and the DGAV-Direção Geral de Agricultura e Veterinária (Portugal; reference 0421/2022 from July 8th, 2022).

**Data availability statement:** The data that support the findings of this study are available in the supplementary material of this article.

**Peer review:** The peer review history for this article is available at <https://publons.com/publon/10.1002/eji.202250206>

## References

- Buszko, M., Nita-Lazar, A., Park, J.-H., Schwartzberg, P. L., Verthelyi, D., Young, H. A., Rosenberg, A. S. Lessons learned: new insights on the role of cytokines in COVID-19. *Nat. Immunol.* 2021. 22: 404–411.
- Urta, J. M., Ferreras-Colino, E., Contreras, M., Cabrera, C. M., Fernández de Mera, I. G., Villar, M., Cabezas-Cruz, A. et al., The antibody response to the glycan  $\alpha$ -Gal correlates with COVID-19 disease symptoms. *J. Med. Virol.* 2021. 93: 2065–2075.
- Villar, M., Urta, J. M., Rodríguez-Del-Río, F. J., Artigas-Jerónimo, S., Jiménez-Collados, N., Ferreras-Colino, E., Contreras, M. et al., Characterization by quantitative serum proteomics of immune-related prognostic biomarkers for COVID-19 symptomatology. *Front. Immunol.* 2021. 12: 730710.
- Villar, M., Urta, J. M., Artigas-Jerónimo, S., Mazuecos, L., Contreras, M., Vaz-Rodrigues, R., Rodríguez-Del-Río, F. J. et al., Correlates with vaccine protective capacity and COVID-19 disease symptoms identified by serum proteomics in vaccinated individuals. *Molecules.* 2022. 27: 5933.
- Chaudhary, J. K., Yadav, R., Chaudhary, P. K., Maurya, A., Kant, N., Rugaie, O. A., Haokip, H. R. et al., Insights into COVID-19 Vaccine development based on immunogenic structural proteins of SARS-CoV-2, host immune responses, and herd immunity. *Cells.* 2021. 10: 2949.
- Ceacareanu, A., Wintrob, Z. P. Summary of COVID-19 vaccine-related reports in the vaccine adverse event reporting system. *J Res Pharm Pract.* 2021. 10: 107–113.
- Adesokan, A., Obeid, M. A., Lawal, A. F. SARS-CoV-2: vaccinology and emerging therapeutics; challenges and future developments. *Ther Deliv.* 2022. 13: 187–203.
- Mohapatra, R. K., Kuppili, S., Kumar Suvvari, T., Kandi, V., Behera, A., Verma, S., Biswal, S. K. et al., SARS-CoV-2 and its variants of concern including Omicron: looks like a never ending pandemic. *Chem. Biol. Drug Des.* 2022. 99: 769–788.
- Li, J., Wang, Y., Liu, Y., Zhang, Z., Zhai, Y., Dai, Y., Wu, Z. et al., Polymorphisms and mutations of ACE2 and TMPRSS2 genes are associated with COVID-19: a systematic review. *Eur. J. Med. Res.* 2022. 27: 1–10.
- Niu, L., Wittrock, K. N., Clabaugh, G. C., Srivastava, V., Cho, M. W. A Structural Landscape of Neutralizing Antibodies Against SARS-CoV-2 Receptor Binding Domain. *Front. Immunol.* 2021. 12: 647934.
- Bangaru, S., Ozorowski, G., Turner, H. L., Antanasijevic, A., Huang, D., Wang, X., Torres, J. L. et al., Structural analysis of full-length SARS-CoV-2 spike protein from an advanced vaccine candidate. *Science.* 2020. 370: 1089–1094.
- Tai, W., He, L., Zhang, X., Pu, J., Voronin, D., Jiang, S., Zhou, Y. et al., Characterization of the receptor-binding domain (RBD) of 2019 novel coronavirus: implication for development of RBD protein as a viral attachment inhibitor and vaccine. *Cell Mol Immunol.* 2020. 17: 613–620.
- Li, W., Moore, M. J., Vasilieva, N., Sui, J., Wong, S. K., Berne, M. A., Somasundaran, M. et al., Angiotensin-converting enzyme 2 is a functional receptor for the SARS coronavirus. *Nature.* 2003. 426: 450–454.
- Yan, R., Zhang, Y., Li, Y., Xia, Lu, Guo, Y., Zhou, Q. Structural basis for the recognition of SARS-CoV-2 by full-length human ACE2. *Science.* 2020. 367: 1444–1448.
- Shi, R., Shan, C., Duan, X., Chen, Z., Liu, P., Song, J., Song, T. et al., A human neutralizing antibody targets the receptor-binding site of SARS-CoV-2. *Nature.* 2020. 584: 120–124.
- Yuan, M., Wu, N. C., Zhu, X., Lee, C.-C. D., Therefore, R. T. Y., Lv, H., Mok, C. K. P. et al., A highly conserved cryptic epitope in the receptor binding domains of SARS-CoV-2 and SARS-CoV. *Science.* 2020. 368: 630–633.
- Yi, C., Sun, X., Ye, J., Ding, L., Liu, M., Yang, Z., Lu, X. et al., Key residues of the receptor binding motif in the spike protein of SARS-CoV-2 that interact with ACE2 and neutralizing antibodies. *Cell Mol Immunol.* 2020. 17: 621–630.
- Wang, P., Nair, M. S., Liu, L., Iketani, S., Luo, Y., Guo, Y., Wang, M. et al., Antibody resistance of SARS-CoV-2 variants B.1.351 and B.1.1.7. *Nature.* 2021. 593: 130–135.
- Starr, T. N., Greaney, A. J., Addetia, A., Hannon, W. W., Choudhary, M. C., Dingens, A. S., Li, J. Z. et al., Prospective mapping of viral mutations that escape antibodies used to treat COVID-19. *Science.* 2021. 371: 850–854.
- Long, S. W., Olsen, R. J., Christensen, P. A., Bernard, D. W., Davis, J. J., Shukla, M., Nguyen, M. et al., Molecular Architecture of Early Dissemination and Massive Second Wave of the SARS-CoV-2 Virus in a Major Metropolitan Area. *mBio.* 2020. 11: e02707–20.
- Hoffmann, M., Arora, P., Groß, R., Seidel, A., Hörnich, B. F., Hahn, A. S., Krüger, N. et al., SARS-CoV-2 variants B.1.351 and P.1 escape from neutralizing antibodies. *Cell.* 2021. 184: 2384–2393.e12.e12.
- Baum, A., Fulton, B. O., Wloga, E., Copin, R., Pascal, K. E., Russo, V., Giordano, S. et al., Antibody cocktail to SARS-CoV-2 spike protein prevents rapid mutational escape seen with individual antibodies. *Science.* 2020. 369: 1014–1018.
- Hansen, J., Baum, A., Pascal, K. E., Russo, V., Giordano, S., Wloga, E., Fulton, B. O. et al., Studies in humanized mice and convalescent humans yield a SARS-CoV-2 antibody cocktail. *Science.* 2020. 369: 1010–1014.
- Shen, X., Tang, H., Mcdanal, C., Wagh, K., Fischer, W., Theiler, J., Yoon, H. et al., SARS-CoV-2 variant B.1.1.7 is susceptible to neutralizing antibodies elicited by ancestral spike vaccines. *Cell Host Microbe.* 2021. 29: 529–539.e3.e3.
- Ferrareze, P. A. G., Franceschi, V. B., Mayer, A. De M., Caldana, G. D., Zimmerman, R. A., Thompson, C. E. E484K as an innovative phylogenetic event for viral evolution: Genomic analysis of the E484K spike mutation in SARS-CoV-2 lineages from Brazil. *Infect. Genet. Evol.* 2021. 93: 104941.
- Melani, R. D., Des Soye, B. J., Kafader, J. O., Forte, E., Hollas, M., Blagojevic, V., Negrão, F. et al., Next-Generation Serology by Mass Spectrometry: Readout of the SARS-CoV-2 Antibody Repertoire. *J. Proteome Res.* 2022. 21: 274–288.



- 27 Goike, J., Hsieh, C. L., Horton, A., Gardner, E. C., Bartzoka, F., Wang, N., Javanmardi, K. et al., Synthetic repertoires derived from convalescent COVID-19 patients enable discovery of SARS-CoV-2 neutralizing antibodies and a novel quaternary binding modality. *Biorxiv*. 2021 [cited 2021 April 9]: 46p. Available from: <https://doi.org/10.1101/2021.04.07.438849>
- 28 Wang, H., Wu, X., Zhang, X., Hou, X., Liang, Te, Wang, D., Teng, F. et al., SARS-CoV-2 Proteome Microarray for Mapping COVID-19 Antibody Interactions at Amino Acid Resolution. *ACS Cent Sci*. 2020. 6: 2238–2249.
- 29 Yi, Z., Ling, Y., Zhang, X., Chen, J., Hu, K., Wang, Y., Song, W. et al., Functional mapping of B-cell linear epitopes of SARS-CoV-2 in COVID-19 convalescent population. *Emerg Microbes Infect*. 2020. 9: 1988–1996.
- 30 Farrera-Soler, L., Daguer, J.-P., Barluenga, S., Vadas, O., Cohen, P., Pagano, S., Yerly, S. et al., Identification of immunodominant linear epitopes from SARS-CoV-2 patient plasma. *PLoS One*. 2020. 15: e0238089.
- 31 Hammel, P., Marchetti, A., Lima, W. C., Lau, K., Pojer, F., Hacker, D., Cosson, P. AI334 and AQ806 antibodies recognize the spike S protein from SARS-CoV-2 by ELISA. *Antib. Rep*. 2020. 3: e186.
- 32 Li, Y., Lai, D.-Y., Zhang, H.-N., Jiang, He-W, Tian, X., Ma, M.-L., Qi, H. et al., Linear epitopes of SARS-CoV-2 spike protein elicit neutralizing antibodies in COVID-19 patients. *Cell Mol Immunol*. 2020. 17: 1095–1097.
- 33 Musicò, A., Frigerio, R., Mussida, A., Barzon, L., Sinigaglia, A., Riccetti, S., Gobbi, F. et al., SARS-CoV-2 Epitope Mapping on Microarrays Highlights Strong Immune-Response to N Protein Region. *Vaccines (Basel)*. 2021. 9: 35.
- 34 Heidepriem, J., Dahlke, C., Kobbe, R., Santer, R., Koch, T., Fathi, A., Seco, B. et al., Longitudinal development of antibody responses in COVID-19 patients of different severity with ELISA, peptide, and glycan arrays: An immunological case series. *Pathogens*. 2021. 10: 438.
- 35 Haynes, W A., Kamath, K., Bozekowski, J., Baum-Jones, E., Campbell, M., Casanovas-Massana, A., Daugherty, P S. et al., High-resolution epitope mapping and characterization of SARS-CoV-2 antibodies in large cohorts of subjects with COVID-19. *Commun Biol*. 2021. 4: 1317.
- 36 Gattinger, P., Niespodziana, K., Stiasny, K., Sahanic, S., Tulaeva, I., Borochova, K., Dorofeeva, Y. et al., Neutralization of SARS-CoV-2 requires antibodies against conformational receptor-binding domain epitopes. *Allergy*. 2022. 77: 230–242.
- 37 Cheng, L., Zhang, X., Chen, Y., Wang, D., Zhang, D., Yan, S., Wang, H. et al., Dynamic landscape mapping of humoral immunity to SARS-CoV-2 identifies nonstructural protein antibodies associated with the survival of critical COVID-19 patients. *Signal Transduct Target Ther*. 2021. 6: 304.
- 38 Qeadan, F., Tingey, B., Gu, L Y., Packard, A. H., Erdei, E., Saeed, An I. Prognostic Values of Serum Ferritin and D-Dimer Trajectory in Patients with COVID-19. *Viruses*. 2021. 13: 419.
- 39 Poudel, A., Poudel, Y., Adhikari, A., Aryal, B. B., Dangol, D., Bajracharya, T., Maharjan, A. et al., D-dimer as a biomarker for assessment of COVID-19 prognosis: D-dimer levels on admission and its role in predicting disease outcome in hospitalized patients with COVID-19. *PLoS One*. 2021. 16: e0256744.
- 40 Nitahara, Y., Nakagama, Yu, Kaku, N., Candray, K., Michimuko, Y., Tshibangu-Kabamba, E., Kaneko, A. et al., High-Resolution Linear Epitope Mapping of the Receptor Binding Domain of SARS-CoV-2 Spike Protein in COVID-19 mRNA Vaccine Recipients. *Microbiol Spectr*. 2021. 9: e0096521.
- 41 Behmard, E., Soleymani, B., Najafi, A., Barzegari, E. Immunoinformatic design of a COVID-19 subunit vaccine using entire structural immunogenic epitopes of SARS-CoV-2. *Sci. Rep*. 2020. 10: 20864.
- 42 Naz, A., Shahid, F., Butt, T. T., Awan, F. M., Ali, A., Malik, A. Designing Multi-Epitope Vaccines to Combat Emerging Coronavirus Disease 2019 (COVID-19) by Employing Immuno-Informatics Approach. *Front. Immunol*. 2020. 11: 1663.
- 43 Moreno-Cid, J A., Pérez De La Lastra, J M., Villar, M., Jiménez, M., Pinal, R., Estrada-Peña, A., Molina, R. et al., Control of multiple arthropod vector infestations with subolesin/akirin vaccines. *Vaccine*. 2013. 31: 1187–1196.
- 44 Almazán, C., Moreno-Cantú, O., Moreno-Cid, J A., Galindo, R C., Canales, M., Villar, M., De La Fuente, J. Control of tick infestations in cattle vaccinated with bacterial membranes containing surface-exposed tick protective antigens. *Vaccine*. 2012. 30: 265–272.
- 45 Aparicio, B., Casares, N., Egea, J., Ruiz, M., Llopiz, D., Maestro, S., Olagüe, C. et al., Preclinical evaluation of a synthetic peptide vaccine against SARS-CoV-2 inducing multiepitopic and cross-reactive humoral neutralizing and cellular CD4 and CD8 responses. *Emerg Microbes Infect*. 2021. 10: 1931–1946.
- 46 European Centre for Disease Prevention and Control [Internet]. Implications of the emergence and spread of the SARS-CoV-2 B.1.1.529 variant of concern (Omicron), for the EU/EEA; 2021 [updated 2021 November 26; cited 2022 October 1]. Available from: <https://www.ecdc.europa.eu/sites/default/files/documents/Implications-emergence-spread-SARS-CoV-2%20B.1.1.529-variant-concern-Omicron-for-the-EU-EEA-Nov2021.pdf>
- 47 Sreepadmanabh, M., Sahu, A. K., Chande, A. COVID-19: Advances in diagnostic tools, treatment strategies, and vaccine development. *J. Biosci*. 2020. 45: 148.
- 48 Majid, S., Khan, M S., Rashid, S., Niyaz, A., Farooq, R., Bhat, S A., Wani, H A. et al., COVID-19: Diagnostics, therapeutic advances, and vaccine development. *Curr. Clin. Microbiol. Rep*. 2021. 8: 152–166.
- 49 Gortázar, C., Del-Río, F. J. R., Domínguez, L., De La Fuente, J. Host or pathogen-related factors in COVID-19 severity? *Lancet*. 2020. 396: 1396–1397.
- 50 Gómez, C. E., Perdiguero, B., Esteban, M. Emerging SARS-CoV-2 variants and impact in global vaccination programs against SARS-CoV-2/COVID-19. *Vaccines (Basel)*. 2021. 9: 243.
- 51 Ijaz, M. K, Nims, R W., Zhou, S. S., Whitehead, K., Srinivasan, V., Kapes, T., Fanuel, S. et al., Microbicidal actives with virucidal efficacy against SARS-CoV-2 and other beta- and alpha-coronaviruses and implications for future emerging coronaviruses and other enveloped viruses. *Sci. Rep*. 2021. 11: 5626.
- 52 Hu, J., Peng, P., Wang, K., Fang, L., Luo, F.-Y., Jin, A.-S, Liu, B.-Z. et al., Emerging SARS-CoV-2 variants reduce neutralization sensitivity to convalescent sera and monoclonal antibodies. *Cell Mol. Immunol*. 2021. 18: 1061–1063.
- 53 Sasson, J M., Campo, J J., Carpenter, R M., Young, M K, Randall, A Z., Trappi-Kimmons, K., Oberai, A. et al., Diverse Humoral Immune Responses in Younger and Older Adult COVID-19 Patients. *mBio*. 2021. 12: e0122921.
- 54 Yadav, P. D., Kumar, S. Global emergence of SARS-CoV-2 variants: new foresight needed for improved vaccine efficacy. *Lancet Infect. Dis*. 2021. 22: 298–299.
- 55 Sayampanathan, A. A., Heng, C. S., Pin, P. H., Pang, J., Leong, T. Y., Lee, V. J. Infectivity of asymptomatic versus symptomatic COVID-19. *Lancet*. 2021. 397: 93–94.
- 56 Oran, D P., Topol, E J. Prevalence of Asymptomatic SARS-CoV-2 Infection. *Ann. Intern. Med*. 2021. 174: 286–287.
- 57 Lovell-Read, F A., Funk, S., Obolski, U., Donnelly, C A., Thompson, R N. Interventions targeting nonsymptomatic cases can be important to prevent local outbreaks: SARS-CoV-2 as a case study. *J. R. Soc. Interface*. 2021. 18: 20201014.
- 58 Wilmes, P., Zimmer, J., Schulz, J., Glod, F., Veiber, L., Mombaerts, L., Rodrigues, B. et al., SARS-CoV-2 transmission risk from asymptomatic

- carriers: Results from a mass screening programme in Luxembourg. *Lancet Reg Health Eur.* 2021. **4**: 100056.
- 59 Sterlin, D., Mathian, A., Miyara, M., Mohr, A., Anna, F., Claër, L., Quentric, P. et al., IgA dominates the early neutralizing antibody response to SARS-CoV-2. *Sci. Transl. Med.* 2021. **13**: eabd2223.
- 60 Aita, A., Basso, D., Cattelan, A. M., Fioretto, P., Navaglia, F., Barbaro, F., Stoppa, A. et al., SARS-CoV-2 identification and IgA antibodies in saliva: One sample two tests approach for diagnosis. *Clin. Chim. Acta.* 2020. **510**: 717–722.
- 61 Thongkum, W., Thongheang, K., Tayapiwatana, C. The occluded epitope residing in Spike receptor-binding motif is essential for cross-neutralization of SARS-CoV-2 Delta variant. *Curr. Issues Mol. Biol.* 2022. **44**: 2842–2855.
- 62 Yarmarkovich, M., Warrington, J M., Farrel, A., Maris, J M. Identification of SARS-CoV-2 Vaccine Epitopes Predicted to Induce Long-Term Population-Scale Immunity. *Cell Rep. Med.* 2020. **1**: 100036.
- 63 He, Y., Li, J., Du, L., Yan, X., Hu, G., Zhou, Y., Jiang, S. Identification and characterization of novel neutralizing epitopes in the receptor-binding domain of SARS-CoV spike protein: revealing the critical antigenic determinants in inactivated SARS-CoV vaccine. *Vaccine.* 2006. **24**: 5498–5508.
- 64 Min, L., Sun, Q. Antibodies and Vaccines Target RBD of SARS-CoV-2. *Front Mol Biosci.* 2021. **8**: 671633.
- 65 Dai, L., Gao, G F. Viral targets for vaccines against COVID-19. *Nat. Rev. Immunol.* 2021. **21**: 73–82.
- 66 Dai, L., Zheng, T., Xu, K., Han, Y., Xu, L., Huang, E., An, Y. et al., A Universal Design of Betacoronavirus Vaccines against COVID-19, MERS, and SARS. *Cell.* 2020. **182**: 722–733.e11.e11.
- 67 Sirohi, P. R., Gupta, J., Somvanshi, P., Prajapati, V. K., Grover, A. Multiple epitope-based vaccine prediction against SARS-CoV-2 spike glycoprotein. *J. Biomol. Struct. Dyn.* 2020. **40**: 3347–3358.
- 68 Artigas-Jerónimo, S., Pastor Comín, J., Villar, M., Contreras, M., Alberdi, P., León Viera, I., Soto, L. et al., A Novel Combined Scientific and Artistic Approach for the Advanced Characterization of Interactomes: The Akirin/Subolesin Model. *Vaccines.* 2020. **8**: 77.
- 69 Contreras, M., Artigas-Jerónimo, S., Pastor Comín, J. J., de la Fuente, J. A quantum vaccinomics approach based on protein–protein interactions. *Methods Mol. Biol.* 2022. **2411**: 287–305.
- 70 De La Fuente, J., Villar, M., Estrada-Peña, A., Olivás, J. A. High throughput discovery and characterization of tick and pathogen vaccine protective antigens using vaccinomics with intelligent Big Data analytic techniques. *Expert Rev. Vaccines.* 2018. **17**: 569–576.
- 71 De La Fuente, J. Translational biotechnology for the control of ticks and tick-borne diseases. *Ticks Tick Borne Dis.* 2021. **12**: 101738.
- 72 De La Fuente, J., Contreras, M. Vaccinomics: a future avenue for vaccine development against emerging pathogens. *Expert Rev. Vaccines.* 2021. **20**: 1561–1569.
- 73 De La Fuente, J., Contreras, M. Additional considerations for anti-tick vaccine research. *Expert Rev. Vaccines.* 2022. **21**: 1019–1021.
- 74 Chen, J.-M. SARS-CoV-2 replicating in nonprimate mammalian cells probably have critical advantages for COVID-19 vaccines due to anti-Gal antibodies: A minireview and proposals. *J. Med. Virol.* 2021. **93**: 351–356.
- 75 La Fuente, J. D., Gortázar, C., Cabezas-Cruz, A. Immunity to glycan  $\alpha$ -Gal and possibilities for the control of COVID-19. *Immunotherapy.* 2021. **13**: 185–188.
- 76 Galili, U. Increasing Efficacy of Enveloped Whole-Virus Vaccines by in situ Immune-Complexing with the Natural Anti-Gal Antibody. *Med Res Arch.* 2021. **9**: 2481.
- 77 Baruah, V., Bose, S. Immunoinformatics-aided identification of T-cell and B-cell epitopes in the surface glycoprotein of 2019-nCoV. *J. Med. Virol.* 2020. **92**: 495–500.
- 78 Maghsood, F., Amiri, M. M., Zarnani, A.-H., Salimi, V., Kardar, G. A., Khoshnoodi, J., Mobini, M. et al., Epitope mapping of severe acute respiratory syndrome coronavirus 2 neutralizing receptor binding domain-specific monoclonal antibodies. *Front Med (Lausanne).* 2022. **9**: 973036.
- 79 Greaney, A J., Loes, A N., Crawford, K H.D., Starr, T N., Malone, K D., Chu, H Y., Bloom, J D. Comprehensive mapping of mutations in the SARS-CoV-2 receptor-binding domain that affect recognition by polyclonal human plasma antibodies. *Cell Host Microbe.* 2021. **29**: 463–476.e6.
- 80 De La Fuente, J., Urra, J. M., Contreras, M., Pacheco, I., Ferreras-Colino, E., Doncel-Pérez, E., Fernández De Mera, I G. et al., A dataset for the analysis of antibody response to glycan alpha-Gal in individuals with immune-mediated disorders. *F1000Res.* 2020. **9**: 1366.
- 81 Pacheco, I., Fernández De Mera, I G., Feo Brito, F., Gómez Torrijos, E., Villar, M., Contreras, M., Lima-Barbero, J. F. et al., Characterization of the anti- $\alpha$ -Gal antibody profile in association with Guillain-Barré syndrome, implications for tick-related allergic reactions. *Ticks Tick Borne Dis.* 2021. **12**: 101651.
- 82 Zhou, P., Yang, X.-L., Wang, X.-G., Hu, B., Zhang, L., Zhang, W., Si, H.-R. et al., A pneumonia outbreak associated with a new coronavirus of probable bat origin. *Nature.* 2020. **579**: 270–273.
- 83 Cheadle, C., Vawter, M P., Freed, W J., Becker, K G. Analysis of microarray data using Z score transformation. *J. Mol. Diagn.* 2003. **5**: 73–81.
- 84 Liu, Y., Hu, G., Wang, Y., Ren, W., Zhao, X., Ji, F., Zhu, Y. et al., Functional and genetic analysis of viral receptor ACE2 orthologs reveals a broad potential host range of SARS-CoV-2. *Proc Natl Acad Sci USA.* 2021. **118**: e2025373118.
- 85 Shang, J., Ye, G., Shi, Ke, Wan, Y., Luo, C., Aihara, H., Geng, Q. et al., Structural basis of receptor recognition by SARS-CoV-2. *Nature.* 2020. **581**: 221–224.
- 86 Lam, Su D, Ashford, P., Díaz-Sánchez, S., Villar, M., Gortázar, C., De La Fuente, J., Orengo, C. Arthropod Ectoparasites Have Potential to Bind SARS-CoV-2 via ACE. *Viruses.* 2021. **13**: 708.
- 87 Studer, G., Tauriello, G., Bienert, S., Biasini, M., Johner, N., Schwede, T. ProMod3 - A versatile homology modeling toolbox. *PLOS Comp Biol.* 2021. **17**: e1008667.

**Full correspondence:** José de la Fuente, SaBio, Instituto de Investigación en Recursos Cinegéticos IREC-CSIC-UCLM-JCCM, Ronda de Toledo s/n, 13005 Ciudad Real, Spain.

Email: jose\_delafuente@yahoo.com; josedejesus.fuente@uclm.es

Received: 11/10/2022

Revised: 19/12/2022

Accepted: 18/1/2023

Accepted article online: 19/1/2023